Title

The systemic anti-microbiota IgG repertoire can identify gut bacteria that translocate across gut barrier surfaces

Journal

Science Translational Medicine, 14(658)

ISSN

1946-6234

Authors

Vujkovic-Cvijin, Ivan
Welles, Hugh C
Ha, Connie WY
et al.

Publication Date

2022-08-17

DOI

10.1126/scitranslmed.abl3927

Peer reviewed

HHS Public Access

Author manuscript

Sci Transl Med. Author manuscript; available in PMC 2023 February 17.

Published in final edited form as:

Sci Transl Med. 2022 August 17; 14(658): eabl3927. doi:10.1126/scitranslmed.abl3927.

The systemic anti-microbiota IgG repertoire can identify gut bacteria that translocate across gut barrier surfaces

Ivan Vujkovic-Cvijin[1,2,*,†], **Hugh C. Welles**[1,2], **Connie W. Y. Ha**[3], **Lutfi Huq**[1], **Shreni Mistry**[2], **Jason M. Brenchley**[4], **Giorgio Trinchieri**[5], **Suzanne Devkota**[3], **Yasmine Belkaid**[1,2,*]

[1]Metaorganism Immunity Section, Laboratory of Immune System Biology, National Institute of Allergy and Infectious Diseases, National Institute of Health, Bethesda, MD, USA.

[2]NIAID Microbiome Program, National Institute of Allergy and Infectious Diseases, Bethesda, MD, USA.

[3]F. Widjaja Foundation Inflammatory Bowel and Immunobiology Research Institute, Cedars-Sinai Medical Center, Los Angeles, CA, USA.

[4]Barrier Immunity Section, Laboratory of Viral Diseases, National Institute of Allergy and Infectious Diseases, National Institute of Health, Bethesda, MD, USA.

[5]Laboratory of Integrative Cancer Immunology, Center for Cancer Research, National Cancer Institute, Bethesda, MD, USA.

Abstract

Unique gut microbiota compositions have been associated with inflammatory diseases, but identifying gut bacterial functions linked to immune activation in humans remains challenging. Translocation of pathogens from mucosal surfaces into peripheral tissues can elicit immune activation, although whether and which gut commensal bacteria translocate in inflammatory diseases is difficult to assess. We report that a subset of commensal gut microbiota constituents that translocate across the gut barrier in mice and humans are associated with heightened systemic immunoglobulin G (IgG) responses. We present a modified high-throughput, culture-independent approach to quantify systemic IgG against gut commensal bacteria in human serum samples without the need for paired stool samples. Using this approach, we highlight several commensal bacterial species that elicit elevated IgG responses in patients with inflammatory bowel disease

[*]Corresponding author. ivan.vujkovic-cvijin@csmc.edu (I.V.-C.); ybelkaid@niaid.nih.gov (Y.B.).

† Present address: Cedars-Sinai Medical Center, Department of Biomedical Sciences, Department of Gastroenterology, F. Widjaja Foundation Inflammatory Bowel and Immunobiology Research Institute, Los Angeles, CA, USA.

Author contributions: I.V.-C. and Y.B. conceived the project. I.V.-C. and L.H. performed all murine experiments. J.M.B. assisted with flow cytometry–based sorting and purification of Ig-coated bacterial fractions. I.V.-C. conceived and designed the SFC, and I.V.-C. and H.W. prepared it. I.V.-C. performed IgA-seq, IgG-seq, and SFC-IgG-seq on human samples. C.W.Y.H. and S.D. performed culture of translocating bacteria in participants with IBD and provided taxon phylogeny information. I.V.-C. performed all bioinformatic analyses. I.V.-C. performed all visualizations of data. Y.B., S.D., and I.V.-C. acquired funding. I.V.-C. wrote the original manuscript, Y.B. and I.V.-C. reviewed and edited the manuscript, and all authors participated in manuscript revisions.

Competing interests: C.W.Y.H. has consulted for Editrix. S.D. has consulted for Reckitt-Benckiser, Interface Bio, GTs Kombucha. The remaining authors declare that they have no competing interests.

SUPPLEMENTARY MATERIALS

www.science.org/doi/10.1126/scitranslmed.abl3927

Figs. S1 to S8

Tables S1 to S6

View/request a protocol for this paper from *Bio-protocol*.

(IBD) including taxa within the clades *Collinsella*, *Bifidobacterium*, *Lachnospiraceae*, and *Ruminococcaceae*. These and other taxa identified as translocating bacteria or targets of systemic immunity in IBD concomitantly exhibited heightened transcriptional activity and growth rates in IBD patient gut microbiomes. Our approach represents a complementary tool to illuminate interactions between the host and its gut microbiota and may provide an additional method to identify microbes linked to inflammatory disease.

INTRODUCTION

Numerous studies have described alterations in the composition of the gut microbiota in the context of disease states (1). However, shifts in relative abundance of gut microbes may not indicate a causal role in pathogenesis. Defined members of the gut microbiota can alter critical functions and exert dominant effects on the community irrespective of their relative abundance (2, 3). Additional efforts to ascertain the impact of the gut microbiota in disease beyond taxonomic relative abundance surveys include metagenomic, metatranscriptomic, and metabolomic studies. However, functional assessment via these approaches remains limited, because substantial proportions of protein-coding gut bacterial genes have no assigned putative function (4, 5) and emergent functions of microbiota gene networks in vivo remain poorly understood. Complementary methods to identify microbes with defined behavior or properties would augment biomedical discovery, especially with regard to microbial functions thought to contribute to disease.

Bacterial translocation from luminal spaces across mucosal barriers has been proposed to contribute to numerous human inflammatory diseases including inflammatory bowel disease (IBD), nonalcoholic steatohepatitis, cancer, HIV-associated comorbidities, obesity (6–9), and responses to immunotherapy (10, 11) and chemotherapy (12, 13). Collectively, these clinical and experimental observations point to bacterial translocation—and the ability of microbes to engage systemic immunity—as a microbial function of relevance to disease. Although advances have been made to identify bacteria in extramucosal internal organs (14), availability of human tissues is limiting, and trace environmental contamination can pose a challenge toward identifying microbes in low-biomass samples (15). On the other hand, the capacity of the adaptive immune system to robustly respond to microbes encountered beyond barrier surfaces could provide a unique opportunity to identify members of the microbiota able to translocate into peripheral tissues and activate systemic immune responses.

Antibodies to gut microbiota members can be quantified using culture-independent molecular techniques (16–20). Such techniques have been successfully used to identify mucosal immunoglobulin A (IgA) against microbiota members and have facilitated identification of gut mucosal adherent bacteria able to spur inflammation in several disease models (16, 17, 20). Secretory IgA is the predominant Ig class expressed at mucosal surfaces and contributes to maintenance of mucosal homeostasis by hindering microbial access to epithelia and promoting commensal bacterial colonization, among other functions (21–25). In the setting of homeostasis, small intestinal resident bacteria comprise most gut microbial targets of mucosal IgA, but mucosal IgA can also be preferentially elicited by ingested

toxins and gut mucosal adherent pathogens (16–18, 20, 26). Studies quantifying and characterizing IgA-bound members of the microbiota underscore how immune responses toward defined members can be a better predictor of microbiota localization or function than shifts in relative abundance. How the presence of other classes of antibodies specific to defined members of the microbiota might uncover privileged modes of interaction and localization remains to be addressed.

Unlike mucosal IgA, systemic IgG is mounted preferentially during systemic inflammatory challenges (27). Systemic IgG antibodies are also characteristically induced after translocation of both gastrointestinal pathogens, e.g., *Trichuris trichiura* (28), *Entamoeba hystolitica* (29), *Salmonella* (30), and gut commensal bacteria, e.g., *Bacteroides fragilis* (31) and commensal *Escherichia coli* (32). Such responses have been shown to confer protection from subsequent challenges as well as from heterologous microbial invasion (32). Whereas commensal gut bacteria can induce systemic IgG at steady state (33, 34), elevated relative systemic IgG against a microbiota member may act as a marker for identification of microbes with enhanced ability for translocation in the context of disease. Whether microbiota member–specific systemic IgG can be probed comprehensively in a high-throughput and unbiased fashion to identify microbes with greater ability to translocate and activate the immune system and whether such a technique can be effective for identifying translocating microbes in humans remain open questions.

Here, we report that translocating murine gut commensal bacteria exhibit heightened targeting by systemic IgG as compared to non-translocating bacterial species. We additionally present a method to quantify anti-microbiota IgG titers in human sera/plasma samples with a surrogate human fecal community from individuals without paired autologous stool, which can readily be applied to already-banked sera from previous human studies. This approach revealed that confirmed translocator bacterial species in a human cohort of patients with Crohn's disease (CD) or ulcerative colitis (UC) exhibited heightened targeting by systemic IgG.

RESULTS

Comparison of human anti-microbiota mucosal IgA and anti-microbiota systemic IgG

We first assessed whether systemic IgG targets different bacteria than those targeted by mucosal IgA. To this end, serum samples and autologous fecal samples from a healthy human cohort were profiled for systemic IgG (IgG-seq) and mucosal IgA (IgA-seq) reactivities using magnetic bead–based separation and 16S ribosomal RNA (rRNA) sequencing of Ig-bound and unbound fecal bacteria ($n = 12$ individuals; Fig. 1, A and B, and fig. S1). IgG and IgA scores were calculated as log ratios of taxon abundances in the bound and unbound fractions. Whereas concordance was evident between IgG and IgA scores, several gut bacterial taxa exhibited greater than 10-fold differences in IgG scores compared to IgA scores (Fig. 1C), indicating differential targeting of taxa by these two Ig classes. Among these differentially targeted taxa, IgA scores correlated more strongly with baseline fecal relative abundances than did IgG scores (Fig. 1, D and E) in our small human cohort, suggesting that bacterium-intrinsic properties independent of the capacity to numerically

dominate the gut influence the elicitation of bacterium-specific systemic IgG more so than mucosal IgA.

Anti-microbiota systemic IgG identifies translocating, proinflammatory bacteria in mice

To better understand the genesis of this heterogeneous bacterial-specific targeting by systemic IgG, we sought to test the hypothesis that systemic IgG reactivity is enriched in specificities directed toward translocating, proinflammatory bacteria. To test this, we used *Toxoplasma gondii*, a well-described model of mucosal infection that is associated with both microbial translocation and increased reactivity toward the microbiota (35, 36). To identify viable microbiota constituents that preferentially translocated across the gut barrier during *T. gondii* infection, mice were orally infected with *T. gondii* and peripheral organs (liver and spleen) were subjected to bacterial culture and identification. A separate group of mice were infected with *T. gondii* and the Ig repertoires were allowed to form over 4 weeks, after which IgA-seq and IgG-seq were performed (Fig. 2A). Gut bacteria that were reproducibly cultured from peripheral organs (among two or more independent experiments, i.e., with a "translocation index" ≥ 2) exhibited differences in IgG scores within mice experiencing *T. gondii*–induced breach of the gut barrier as compared to uninfected mice (Fig. 2B and table S1). This observation was not evident when examining mucosal IgA (Fig. 2B), suggesting that elevated IgG could be a potential marker for translocating microbes. Furthermore, when administered to mice before *T. gondii* infection, IgG-targeted bacteria elicited heightened markers of blood T cell activation compared to bacteria that were not differentially targeted by IgG in *T. gondii*–infected mice (fig. S2, A to D), suggesting that IgG-targeted bacteria could have proinflammatory properties.

The relative concordance between the mucosal IgA and systemic IgG anti-microbiota repertoires in our cohort of healthy individuals (Fig. 1), which was consistent with previous reports (19, 34), prompted us to examine relationships between these two repertoires under conditions of homeostasis and disease. Gut barrier disruption and chronic inflammation as induced by *T. gondii* or *Yersinia pseudotuberculosis*, a bacterial pathogen that induces bacterial translocation (37), caused divergence of the systemic IgG and mucosal IgA repertoires compared to uninfected healthy mice ($P = 0.013$ for *T. gondii* model and $P = 0.093$ for *Y. pseudotuberculosis*; fig. S2E).

A surrogate fecal community for profiling human serum samples for microbiota reactivity

Mice and humans exhibit substantial differences in gut microbiota composition, and key immunomodulatory gut bacteria found in mice are absent in humans (38, 39). This highlights the importance of developing scalable research tools that can be applied to human samples using readily available sample sources. Availability of paired serum and stool samples is limited. To overcome this important hurdle, we developed a modified IgG-seq procedure using human serum samples in conjunction with a surrogate fecal community (SFC), which was used in place of autologous paired stool (Fig. 3A). This SFC was designed to contain the greatest number of unique bacterial taxa possible from a combination of stool samples derived from healthy donors to ensure probing the greatest number of taxa for serum IgG reactivity. This was accomplished by first applying 16*S* rRNA sequencing to 40 healthy human volunteer stool samples. The combination of stool samples that yielded the

community with maximal diversity was subsequently calculated using Monte Carlo–based in silico modeling (fig. S3A). Fifteen healthy human volunteer stool samples were then combined and used as the SFC for subsequent analyses. The resulting SFC encompassed 8 phyla, 13 classes, 17 orders, 33 families, 84 genera, and 1876 unique amplicon sequence variants (ASVs) of human gut bacteria (fig. S3B). Human serum samples were incubated with this SFC, and IgG-unbound taxa were removed by magnetic bead–based separation (fig. S4, A and B). When comparing IgG scores using the SFC (by the SFC-IgG-seq method) to IgG scores obtained using paired serum and stool samples (by the IgG-seq method) in the same cohort, there was significant, nonrandom concordance between the two methods (two-sided z test $P = 4.37 \times 10^{-9}$; fig. S4, C and D) that was unlinked to total serum IgG (fig. S4E). Furthermore, IgG scores derived from SFC-IgG-seq were compared to bacterium-specific serum IgG quantities, as quantified by a flow-based assay performed on pure cultures of a bacterial isolate (40). Relative concordance between the two measures was described when assessing IgG against *Megasphaera massiliensis* when the bacterium was cultured in vitro ($P = 0.034$, Spearman rho = 0.32; fig. S4F). Stronger concordance between *M. massiliensis* SFC-IgG-seq scores and antibacterial IgG was found when bacteria were obtained from feces of gnotobiotic mice monocolonized with *M. massiliensis* compared to *M. massiliensis* cultured in vitro ($P = 0.000051$, Spearman rho = 0.58; fig. S4E). This was in agreement with observations that certain cell surface microbial antigens are expressed preferentially in vivo and suppressed in vitro (23, 41).

Antimicrobiota systemic IgG identifies translocating bacteria in the human gut microbiota

To understand whether systemic IgG could be useful as a marker to facilitate identification of translocating gut bacteria in humans, we applied SFC-IgG-seq to a cohort of patients with IBD who underwent ileal or colonic surgical resection and to a cohort of healthy controls (patient characteristics in tables S2 and S3). Mesenteric adipose tissue from patients with IBD was subjected to bacterial culture as a way to identify taxa that had translocated across the gut barrier and entered the mesentery (Fig. 3B) (42). Recovered bacterial isolates were identified by full-length 16*S* rRNA sequencing, as previously reported (42). Translocating bacteria that were isolated from mesenteric adipose tissue from more than four individuals were considered for downstream analyses. We sought to test whether the translocation of such bacteria in a given individual was associated with heightened cognate systemic IgG responses. We compared IgG scores for patients with IBD for which bacterial translocation was confirmed by culture to IgG scores for patients with IBD for whom bacterial translocation was not observed. When aggregating data for translocating bacteria, a significant increase in IgG scores was seen in translocation-positive individuals compared to translocation-negative individuals ($P = 0.0268$; Fig. 3C). Given that IBD disease exhibits dynamic and fluctuating severity within individuals over time, it is possible that the time of mesenteric sampling missed some bacterial translocation events. Thus, we analyzed IgG score dynamics for translocating bacteria among a third control group of healthy individuals. We observed a significant stepwise increase in IgG scores among these healthy participants, translocation-negative patients with IBD, and translocation-positive patients with IBD ($P = 0.00015$; Fig. 3C) when considering all translocating bacteria. Individual translocating bacterial taxa that exhibited significant linear increases in IgG scores from healthy, to IBD translocation-negative, to IBD translocation-positive individuals included *Bifidobacterium*

longum, *Collinsella aerofaciens*, and *Bacteroides vulgatus* ($P = 0.00062$, $P = 0.00072$, and $P = 0.014$, respectively; fig. S5). To understand whether mucosal abundance alone explained heightened IgG scores for detected taxa, we examined correlations between IgG scores and mucosal relative abundances, as detected by 16*S* rRNA profiling of mucosal biopsies from the same cohort of individuals with IBD. Such correlations were generally weak and exhibited a random distribution (fig. S6A), supporting the idea that IgG scores are nonredundant with gut mucosal relative abundance. Small intestinal residency of a gut bacterium may be sufficient to induce mucosal IgA (18). Thus, we examined whether the presence of each taxon at the mucosa, assessed by 16*S* rRNA gene sequencing of intestinal biopsies, affected observations of heightened systemic IgG in translocation-positive patients with IBD. When examining only those individuals with a detectable mucosal presence of a given translocating bacterium, the observation that translocating bacteria exhibited heightened IgG scores in patients with IBD with confirmed bacterial translocation compared to patients with IBD without bacterial translocation remained evident ($P = 0.0142$; fig. S6B).

The antimicrobiota systemic IgG repertoire differs between patients with IBD and healthy controls

IBD, which encompasses CD and UC, is characterized by breach of the gut barrier and immune activation. This immune activation is a critical driver of disease progression and is thought to be stimulated and amplified by the gut microbiota. Proportions of fecal bacteria that are endogenously coated with IgG are heightened in both CD and UC (43–47), and this measure correlates strongly with disease activity (48, 49). However, the specific identities of IgG-targeted bacteria in IBD and what such IgG targeting of gut microbiota constituents may indicate with regard to gut bacterial functions remain poorly understood. Consistent with previous observations (43–49), our analysis revealed that a greater proportion of bacteria in the SFC was targeted by IgG in IBD serum compared to serum IgG from healthy controls (Fig. 4A). Using SFC-IgG-seq, we examined IgG targeting of all detectable taxa within the SFC, first comparing total antimicrobiota IgG repertoires between groups. Antimicrobiota IgG repertoires of patients with IBD clustered separately from those of healthy individuals [$P = 0.0056$, permutational multivariate analysis of variance (PERMANOVA); Fig. S7A], a finding that was robust for both CD and UC separately ($P = 0.011$ and $P = 0.026$, respectively, PERMANOVA; Fig. 4, B and C). This segregation by antimicrobiota IgG repertoires was independent of concurrent medications, physiological factors, and lifestyle factors when examining all individuals (table S4). Numerous specific taxa were found to be preferentially targeted by IgG in serum samples from patients with CD and patients with UC compared to serum from healthy controls (Fig. 4, D to F). *Lachnospiraceae* and *Ruminococcaceae* members were among the principal targets of systemic IgG in sera from patients with IBD by both nonparametric (Fig. 4, D to F) and compositional statistics (fig. S7B and table S5). Systemic IgG responses mounted against microbial antigens can have cross-reactivity against structurally related antigens such as those from phylogenetically related taxa (32). Such off-target responses are typically weaker than those directed at the immunogen (50, 51), and thus, taxa with the greatest group-wise differences in IgG scores are more likely to be true targets of IgG. Such taxa included those that had confirmed culture-positive translocation in patients with IBD (*B. longum* and *C. aerofaciens*) and others that had more fastidious culture requirements

but exhibited robust differences in IgG scores (*Faecalibacterium prausnitzii* and *Blautia wexlerae*; Fig. 4, G to J). Antimicrobiota IgG repertoires segregated patients with CD from controls more strongly than patients with UC from controls ($F = 2.121$ versus $F = 1.78$; Fig. 4, B and C). In line with this observation, most taxa that differed in their IgG scores between patients with CD and patients with UC exhibited heightened IgG scores in patients with CD (fig. S7C), suggesting heightened IgG targeting of gut microbiota members in CD compared to UC.

Gut microbe transcriptional activity and growth rates are increased for translocating taxa targeted by IgG

Efforts to characterize bacterial functions in human microbiome studies include the assessment of human gut commensal bacterial growth rates using metatranscriptomics and metagenomics. Such studies have revealed differences in proliferative activity of specific taxa in healthy individuals compared to individuals with different diseases (52). However, the behavior of bacteria that exhibit differential growth patterns and whether such bacteria engage in privileged interactions with their host remain poorly understood. We focused on CD, given greater IgG profile differences, and data were examined from the longitudinal integrative Human Microbiome Project (iHMP) consortium (53). Taxa were ranked by the strength of correlation between the extent of gut dysbiosis in patients with CD and the overall transcriptional rate (RNA/DNA ratio) of each taxon (Fig. 5A), a measure that has been linked to bacterial activity (54) and growth rate (55). Taxa whose transcriptional rate correlated with dysbiosis overlapped with taxa identified by IgG-seq (in Fig. 4D) or identified as translocating species after culture (in Fig. 3B). Specifically, in the iHMP dataset, we examined taxa that we confirmed as translocating species in our cohort (highlighted in yellow, Fig. 5), taxa that exhibited heightened IgG scores in sera of our patients with CD (purple, Fig. 5), and taxa that were both confirmed translocators and exhibited heightened IgG (red, Fig. 5). Several taxa that fell within these three categories were represented among the top 10 taxa whose transcriptional rate (RNA/DNA ratio) correlated most closely with dysbiosis in the iHMP dataset (Fig. 5A).

Bacterial growth rates can be inferred from metagenomic sequencing studies via the quantification of peak-to-trough ratios (PTR), which measure the ratio of reads near a bacterial origin of replication compared to reads at the replication terminus (52, 56). In two independent cohorts of CD and healthy individuals from separate continents (57, 58), we compared bacterial growth rates of all detected gut taxa between CD and healthy individuals. Concordant with the analysis of bacterial activity by transcription rate, several taxa that were translocating species or exhibited heightened IgG in our cohort of patients with CD overlapped with those exhibiting increased bacterial growth rates assessed by PTR (Fig. 5, B and C). *B. longum*, which was a prominent translocator and target of systemic IgG in our IBD cohort, exhibited higher bacterial activity/growth rates in all three independent datasets queried (Fig. 5, A to C). *C. aerofaciens* was also a prominent translocator and target of systemic IgG and showed higher activity/growth rates in two of three datasets (Fig. 5, A and B). *Tyzzerella nexilis*, a confirmed translocator in our IBD cohort, was also among the top species exhibiting higher growth rates in two of three datasets (Fig. 5, B and C).

In comparison to analyses examining differential bacterial growth rates in CD compared to healthy individuals, relative abundance analyses yielded lists of differentially abundant taxa that had comparatively less representation of translocators and bacterial targets of IgG (Fig. 5, D to F). Taxa that were confirmed translocators or exhibited heightened systemic IgG in CD were rarely identified by differential abundance analyses (seven instances) and exhibited mixed directional results with nearly equal numbers of taxa being enriched in CD as enriched in healthy controls (Fig. 5H). On the other hand, when examining the top taxa with differences in bacterial growth rates between patients with CD and healthy controls, bacteria that were translocators or exhibited higher IgG scores were represented in 15 instances, with 14 of 15 exhibiting uniformly higher bacterial growth rates in CD (Fig. 5G). Thus, translocators and proinflammatory gut bacteria in our CD cohort were more represented among the taxa identified by differential bacterial growth rate analyses than those by relative abundance analyses ($P = 0.032$, χ^2 test) when comparing patients with CD to healthy controls. This was also evident when examining the taxa among the three studies filtered by P value ($P < 0.05$, Mann-Whitney test) and Benjamini-Hochberg false discovery rate (Q value < 0.05; fig. S8). By these two data filtration criteria, bacterial activity/growth rates had greater consistency in identifying IgG-targeted or translocating bacteria than did increases in relative abundance ($P = 0.00083$ for P value cutoff and $P = 0.033$ for Q value cutoff, by Fisher exact test). There was also a proportional enrichment for IgG-targeted or translocating bacteria in the lists of taxa with differential growth rates as compared to taxa with differential abundance ($P = 0.00016$ for P value cutoff and $P = 0.019$ for Q value cutoff, by Fisher exact test). These data suggest that heightened bacterial activity/growth rate in CD is a trait that overlaps with heightened bacterium-specific IgG responses and the functional capacity of microbes to translocate across the gut barrier.

DISCUSSION

Here, we report that increases in gut commensal bacterium-specific systemic IgG were observed for bacteria that had translocated across the gastrointestinal tract in mice and humans. We show that profiling of the antimicrobiota systemic IgG repertoire could be leveraged to identify translocating bacteria in the context of human disease. We found that gut bacterium-targeted systemic IgG and mucosal IgA repertoires diverged in the setting of gut barrier disruption and that the systemic IgG repertoire shifted toward translocating gut bacteria and taxa that can be proinflammatory in the setting of gut barrier disruption. In both UC and CD, heightened systemic IgG responses were detectable against several gut taxa including those within the *Bifidobacterium*, *Collinsella*, *Faecalibacterium*, and *Blautia* genera, suggesting preferential translocation of these taxa in IBD. As bacterial translocation in immunocompetent hosts is met with immune activation, the principal driver of IBD pathology, this microbial activity may be relevant to disease progression and translocating bacteria could represent a viable therapeutic target. High *Collinsella* and *Bifidobacterium* spp. abundance has been associated with a positive response to anti–tumor necrosis factor therapies, suggesting a link between these bacteria and this pathologic innate inflammatory pathway (59). Furthermore, increased *Collinsella* was uniquely associated with the likelihood of developing severe, penetrating disease in a pediatric CD cohort (60). *Bifidobacterium adolescentis* induces small intestinal T helper 17 (T_H17) cells (61, 62)

and *B. longum* potently induces type 3 innate lymphoid cells in the small intestine (61), cell types implicated in IBD pathology (63, 64). In our small cohort, patients with CD exhibited greater IgG targeting of gut commensals than did patients with UC. Taxa with heightened IgG responses in patients with CD or those detected as translocating across the gut barrier in CD also exhibited greater activity and proliferation across three independent metagenomic and metatranscriptomic datasets, suggesting a link among increased overall bacterial activity, capacity for translocation, and targeting by IgG.

Not all translocating bacteria in our study were associated with increased bacterium-specific IgG in sera from patients for which bacterial translocation was confirmed. It is possible that such gut bacteria have evolved immune evasion strategies (65) or that they may translocate over the lifetime of a healthy individual to a sufficient extent that a plateau of maximal specific IgG was induced in both cases and controls. *Enterobacteriaceae* have been found in mesenteric lymph nodes of both healthy controls and patients with IBD (66, 67), which may explain why those with verified translocation of *E. coli* did not exhibit heightened IgG scores for *E. coli* compared to those without verified *E. coli* translocation. Alternately, induction of IgG against a specific bacterial strain that shares its V4 16*S* rRNA sequence with other nonimmunogenic strains may limit capacity of 16*S* sequencing-based IgG-seq methods to identify preferentially IgG-targeted taxa. This may also be the case for *E. coli*, a species that includes numerous nonpathogenic commensal strains in humans and invasive, highly inflammatory strains that share the same V4 16*S* rRNA sequence. Thus, a lack of increased IgG against *E. coli* and other taxa may be due to insufficient resolution of V4 16*S* rRNA sequencing, preventing disambiguation of commensal *E. coli* from related pathogenic taxa. The observation of nonzero IgG targeting of a bacterium also does not necessarily denote translocation. Commensal microbiota members can induce antigen-specific IgG at steady state, independently of confirmed translocation as in the case of *Akkermansia muciniphila* (33). Accordingly, we observed that serum IgG repertoires bound to large proportions of the gut bacterial community even in healthy humans. Approaches such as SFC-IgG-seq, which involve comparison of antimicrobiota IgG repertoires in those with gut barrier disruption compared to controls without presumed bacterial translocation, are likely to help discern steady-state IgG production against a bacterium from that of IgG mounted in response to bacterial translocation. Such systemic IgG may not only serve as a defense against future bacterial translocation events but also play an as-yet undefined role in the host-microbiota relationship including mutualistic effects. Further characterization of antimicrobiota antibody repertoires may help to illuminate the basis of the privileged modes of interaction that IgG-targeted bacteria may have with their host, which may be of particular importance in the setting of inflammatory disease.

Although we specifically examined mice and humans with major gut barrier disruption, low-affinity T cell–independent IgA and IgG that are broadly reactive to most gut commensal microbes have been observed during health and immune homeostasis (18, 19). Such homeostatic responses may be induced by qualitatively different host-microbe interactions than those highlighted in the present study. Group comparisons between individuals with gut barrier disruption and healthy individuals may allow discrimination of bacteria associated with IgG responses that surpassed the threshold for homeostatic antibody induction. Examination of different antibody isotypes and multimerization states may facilitate finer

discrimination of different modes of host-microbial interactions. For example, serum IgA, which differs structurally from secretory IgA expressed at the mucosa, is robustly induced by systemic inflammatory stimuli (68, 69) such as serum IgG and can also protect from lethal bacteremia (70). Further investigation into the role of secretory compared to serum IgA is warranted and may provide another lens by which to understand host-microbe immune relationships. In addition, we observed that the antimicrobiota mucosal IgA and systemic IgG repertoires were largely concordant in mice during homeostasis, mirroring results of previous studies (19, 34). Inflammatory stimuli that disrupt the gut barrier and promote chronic inflammation (*T. gondii* and *Y. pseudotuberculosis*) caused a divergence in the mucosal IgA and systemic IgG antimicrobiota repertoires, with the IgG repertoire becoming skewed toward microbes that had translocated in our murine experiments. Whether the same occurs in humans who experience gut barrier disruption and whether antibody isotypes differ in their interrelationships remain to be elucidated.

Mucosal IgA induction can promote a mutualistic host-microbial relationship by limiting pathogenic functions such as motility (41) and by inhibiting expression of pathogenesis-associated macromolecular structures such as hyphae (71) and flagella (72). In contrast to the healthy state, patients with IBD exhibit antimicrobiota IgG present in the gut lumen (43–47), and thus, it is possible that systemic IgG directly modulates gut bacterial functions in a mutualistic manner analogous to IgA in that setting. On the other hand, IgG-opsonized gut microbes can spur colitis as a result of an imbalance in activating Fc receptors on myeloid cells (49), and thus, even such host-mediated mutualistic pruning of bacterial function may contribute to inflammatory pathology. Given our observation of IgG targeting of *Lachnospiraceae* members, which have been associated with protection from colitis (73, 74), possible proinflammatory properties of some IgG-targeted bacteria may be outweighed by their beneficial effects. Such beneficial effects may include production of short-chain fatty acids, a metabolic function that is highly enriched among *Lachnospiraceae* (75) and induces anti-inflammatory regulatory T cells (76, 77). Whereas our data support the hypothesis that elevated systemic IgG against a gut bacterium can be indicative of certain bacterial functions (i.e., propensity to translocate), whether such functions dominantly contribute to disease remains to be explored. Further mechanistic work to better understand the complex role of such bacterial functions, and resulting host immune responses to these functions, in disease is warranted.

There are a number of limitations to our study. Limitations to profiling Ig reactivities as a method to identify biologically relevant microbiota constituents include the phenomenon of cross-reactivity. In the context of systemic immune engagement with a translocating microbe, cross-specific antibody induction may occur and contribute to elevation of IgG against structurally related antigens such as those from phylogenetically related taxa that did not translocate. In studies examining such processes, systemic antibodies exhibit greater propensity for binding to the primary immunogen than to heterologous antigens (78, 79). Thus, we placed emphasis on the top taxa exhibiting differential IgG scores between cases and controls with the expectation that the true immunogen would have increased IgG targeting and that taxa targeted by nonspecific cross-reactive antibodies would have comparatively smaller differences in IgG scores between cases and controls. Through the intentionally designed microbial complexity of the SFC, we attempted to maximize the

likelihood that the original immunogen was present in this community and, thus, that the relevant IgG targets could be identified. However, the immunogen may be expressed by an especially rare taxon or one absent from the SFC, and thus, possible cross-reactivity without detection of the original immunogen-bearing taxon cannot be ruled out. This may be especially so for *Enterobacteriaceae* members, a clade that is composed of both pathogens and commensals. We did not include feces from individuals with infectious gastrointestinal disease in our SFC, making it unlikely that our SFC facilitates measurement of IgG titers to bona fide pathogens that may be the original immunogens of some cross-targeted taxa. Recent peptide array–based serum IgG repertoire profiling advances are likely to overcome such limitations, in that they can quantitate IgG against peptide epitopes of common pathogens (80). Our approach benefits from quantifying IgG against microbial antigens because they are seen by the immune system in vivo, with complex tertiary and quaternary structure as well as glycan and glycolipid moieties, and a combination of such approaches is likely to yield new insights. Furthermore, IgG targeting of taxa in severe IBD as performed in our study may be the result of bystander inflammation that is secondary to disease-related inflammatory pathology. Thus, elevated IgG against a microbe cannot be definitive evidence for translocation of that bacterium or for proinflammatory potential but, instead, may aid in narrowing the list of microbes with these suspected properties in a given condition. Last, genetic risk alleles associated with IBD may alter IgG responses to gut microbes, and thus, the observation of heightened or lowered IgG responses in a disease may reflect underlying genetic differences as opposed to differences in levels of bacterial translocation.

The method developed in the present study to identify bacteria targeted by systemic IgG yielded information that was nonredundant with that of relative abundance comparisons, providing an additional tool in the pursuit of identifying causally related microbiota constituents in disease. Specifically, quantifying IgG against gut microbiota members using the IgG-seq technique as presented herein facilitated the identification of gut bacteria that harbored the discrete function of having translocated across the gut barrier. Comparing IgG scores for all gut bacteria between healthy controls and patients with IBD revealed a repertoire of antimicrobiota immune responses that was unique to IBD, highlighting taxa with privileged modes of interaction with host immunity in this disease. Future examinations comparing patients with CD to patients with UC in larger, balanced cohorts and patients with CD with disease localized to different parts of the gut are likely to yield insights into unique host immune-microbiota relationships as a function of disease type. Furthermore, our population of patients with IBD exhibited severe manifestations of disease, requiring surgical interventions. Thus, examination of patients with IBD across a spectrum of disease severity will reveal whether gradations of IgG titers against the specific taxa identified here may manifest differently depending on disease severity and putative disease subtypes.

The SFC-IgG-seq technique using an SFC as presented here can be used on existing serum samples to identify gut microbiota members that may translocate across the gut barrier in human inflammatory disease, without the need for stool sampling. Using a single combined stool substrate per participant obviates variability in comparative gut microbiota studies that is inherent to human stool, including intraindividual temporal variability and intrafecal spatial variability (81). Thus, examining immune responses to a fixed SFC can reduce noise attributable to certain sources of variability in human microbiota

studies. Mining host immune memory to better understand microbiota member function and behavior as presented here may help to illuminate therapeutic targets for the amelioration of immunopathology.

MATERIALS AND METHODS

Study design

The objective of this study was to investigate whether antimicrobiota antibodies can yield biological information about gut bacterial functions relevant to human disease. Focusing on bacterial translocation as a bacterial function of interest, murine experiments were performed in which translocation of gut commensal bacteria was experimentally induced using infections with *T. gondii* and *Y. pseudotuberculosis*. Human antimicrobiota antibody responses in the form of mucosal IgA and systemic IgG were investigated using human fecal and plasma samples from healthy volunteers. To investigate the effects of bacterial translocation on human antimicrobiota systemic IgG repertoires, serum from patients with IBD who underwent surgical bowel sampling and bacterial translocation characterization was queried.

Mice were male C57BL/6J-CD45a(Ly5a) obtained from Taconic Biosciences, ages 3 to 7 weeks, and each experiment used mice of the same age and shipment. Experimental groups were randomly assigned but without investigator blinding. Murine experiments were each performed on three independent occasions, and animals were only excluded in the case of failed 16*S* rRNA amplification of both positive and negative fractions of IgG-seq or IgA-seq experiments.

Each SFC-IgG-seq participant sample was assayed in duplicate; two wells of SFC were incubated with each human participant plasma sample and were processed as described below. Human serum samples for SFC-IgG-seq were randomly distributed throughout the 96-well plate so as to minimize possible sources of bias. The initial healthy human cohort ($n = 12$) with paired serum and stool samples was used for discovery purposes to examine differences between antimicrobiota IgA and IgG profiles and was obtained from the Consortium for the Evaluation and Performance of HIV Incidence Assays (CEPHIA) of the University of California, San Francisco. The subsequent human cohort ($n = 38$) with only serum samples was used to address the hypothesis that translocating bacterial species could be identified by their IgG titers and included healthy individuals and patients with CD or UC. Human serum samples were from the Cedars-Sinai Medical Center. All study participants provided informed consent for participation in research as part of the ongoing MIRIAD (Material and Information Resources for Inflammatory and Digestive Diseases) Biobank program of the F. Widjaja Foundation Inflammatory Bowel and Immunobiology Research Institute (Institutional Review Board no. 3358). Blinding was not performed, and investigators were aware of the bacterial translocation metadata for serum samples so as to perform the analyses described.

IgA-seq and IgG-seq on paired human serum and stool samples

Stools and sera from 12 healthy human donors who provided informed consent were obtained, and IgA-seq and IgG-seq were performed simultaneously (referring to data shown in Fig. 1). Sera were heat-inactivated at 56°C for 35 min to block complement activity and were diluted to 1:500. Stool (200 mg) was weighed on dry ice and resuspended in 1% bovine serum albumin (w/v) in phosphate-buffered saline (PBS), a solution used for all subsequent staining, washing, and resuspension steps. Suspensions were centrifuged at 200 relative centrifugal force (rcf) for 1 min to pellet food particles. Each sample input was adjusted to have equivalent OD_{600} (optical density at 600 nm), and five separate aliquots were taken: two to be incubated with serum for IgG-seq, two for mucosal IgA-seq (without serum incubation), and one for pre-enrichment 16*S* rRNA sequencing. One aliquot from each pair of aliquots was used for isotype staining, whereas the other was used for downstream fractionation and analyses. Aliquots for IgG staining were incubated with paired sera from the same individual for 30 min at 4°C. Samples were washed, with all centrifugation steps being performed at 8000 rcf for 3 min. Serum-incubated samples were stained with anti-IgG phycoerythrin (PE) (1:50 dilution; Miltenyi Biotec, #130093193) and SYTO-62 (1:500 dilution; Invitrogen), which stains bacterial cells, and samples for IgA-seq were stained with anti-IgA PE (1:40 dilution; Miltenyi, #130093128) for 20 min at 4°C. Aliquots of each stained sample were taken for flow cytometry assessment of quality of staining. Flow cytometry was performed on an LSRII (Beckton-Dickinson) machine with thresholds set to 200 on the side-scatter parameter to facilitate capture of bacterial events. Total IgG concentrations in serum samples were quantified using the IgG Human ELISA Kit (Invitrogen, #BMS2091).

Samples were then subjected to magnetic column-based separation using anti-PE microbeads (Miltenyi, #130-048-801) at a concentration of 1:20, and subsequent steps were followed as per manufacturer protocol, and the Ig eluate was collected and spun by centrifugation to remove excess buffer before freezing. To increase the degree of Ig^+ cell enrichment, the Ig^+ fraction was subjected to additional column enrichment. The column used for the first enrichment was washed by passing ethanol through the column with a plunger followed by PBS, and the Ig^+ sample was then applied, and the manufacturer protocol was again performed. The final Ig^+ fraction was centrifuged, excess buffer was removed, and the pellet was frozen for downstream processing.

DNA was extracted from samples using the MagAttract Power-Microbiome DNA/RNA Kit (QIAGEN). Amplification of the V4 16*S* rRNA gene (primers 515f and 806r) was performed in accordance with the Illumina-recommended protocol, and amplicons were purified using AMPure XP beads (Beckman Coulter), quantified using the KAPA Quantification Kit (Roche), and pooled at equimolar concentrations. Pooled libraries were sequenced on a MiSeq instrument (Illumina).

Sequencing analysis was performed as follows: ASV tables were constructed using Dada2 (82) in the R programming environment. ASVs with fewer reads than 0.01% of total reads and those detected in fewer than 10% of samples were filtered out. ASV tables were rarefied at 11,000 sequences per sample. IgA and IgG scores were calculated as the $\log_{10}$ ratio counts of each taxon in the Ig-bound microbial fraction over the counts in the Ig-unbound

microbial fraction. To understand the basis of differences in IgA targeting or IgG targeting of ASVs, ASVs that exhibited greater than 10-fold differences in IgA versus IgG scores were selected. Analyses were further confined to taxa that had nonzero targeting by Igs by selecting ASVs with average Ig scores greater than zero across all individuals. IgG or IgA scores for each resulting ASV were then compared to baseline pre-enrichment ASV relative abundances across all individuals using Spearman correlation tests (R package "Hmisc").

T. gondii infection of mice

An ME-49 clone of *T.* gondii transfected with red fluorescent protein was obtained from M. Grigg [National Institute of Allergy and Infectious Diseases/National Institutes of Health (NIAID/NIH)], which was used for cyst production in wild-type C57BL/6 mice and for cyst quantification via fluorescence microscopy. Tissue cysts were obtained from brains of orally infected mice, were physically dissociated via repeated passage through 19-gauge needles, and were resuspended in PBS. Experimental mice were infected with eight cysts via oral gavage. All animal experiments were performed in accordance with guidelines from the NIH Animal Care and Use Committee.

Identification of translocating bacteria from culturing murine organs

Spleens, livers, and brains (as negative controls) from *T. gondii*–infected mice were excised using autoclaved forceps and scissors and were transferred to prereduced anaerobic transport medium tubes (Anaerobe Systems, #AS-911) before transfer to an anaerobic chamber. Tissues were subsequently physically disrupted and filtered through sterile 40-μm filters using prereduced anaerobic PBS. Resulting suspensions were plated on YCFAC+B (Anaerobe Systems, #AS-677), MTGE (Anaerobe Systems, #AS-777), and Columbia Blood Agar (Thermo Fisher Scientific, #R01217) at 37°C for 48 to 72 hours. A set of Columbia Blood Agar plates was also incubated in aerobic conditions at 37°C for 48 to 72 hours. Brain tissue was cultured as a negative control, as were buffers in which tools were dipped before organ resection, both of which routinely yielded no colonies. Colonies were propagated for 48 hours at 37°C in liquid medium corresponding to that from which they were grown, were cryopreserved, and were identified by full-length 16*S* rRNA Sanger sequencing. Translocator culture was performed during three independent experiments with 5 to 10 mice infected with *T. gondii* being subjected to culture each time, with 1 to 2 uninfected control mice to test for negative culture plates. Culture of translocator bacteria from mesenteric adipose tissue of human participants undergoing surgical resection was performed as described previously (42).

IgG-seq and IgA-seq on *T. gondii*–infected mice

Sera and stool were collected from mice 4 weeks after infection with *T. gondii* and frozen as part of three independent experiments with 5 to 10 mice per group (infected and uninfected). Stools were placed in buffer [1% (w/v) bovine serum albumin in PBS, used for all subsequent washing and staining steps], were physically disrupted using sterile pipette tips, and were homogenized by repeated pipetting using wide-bore pipette tips by pipetting. Stool suspensions were spun at 50 rcf for 1 min to pellet nonbacterial food particles. Supernatant was passed through a 40-μm filter to a new sterile tube and was washed by centrifugation at 8000 rcf for 3 min (same speed and time for subsequent washes). One-tenth of this

suspension was used to quantify OD_{600} for normalization of input samples. Another 1/10 of this suspension was set aside for flow cytometry–based assessment of percentages of pre-enrichment IgA and IgG fecal bacterial binding. Samples were split for IgA-seq and IgG-seq. Samples for IgG-seq were incubated in 1:50 plasma for 30 min at 4°C, whereas samples for IgA-seq rested at 4°C. Samples were resuspended in stain mixtures including SYTO-62 (1:500 dilution; Invitrogen), anti-IgA (dilution 1:40; PE, eBioscience, clone:11-44-2) for IgA-seq samples, and anti-IgG1 PE (1:300; Beckton-Dickinson, #550083), anti-IgG2ab PE (1:20; Beckton-Dickinson, #340269), anti-IgG3 PE (1:1500; Santa Cruz Biotechnology, #sc-3767) for IgG-seq samples. All stains were performed for 15 min at 4°C. Stains were simultaneously performed using isotype control antibodies conjugated to PE, which yielded minimal to no staining for all experiments. Samples were subsequently washed and subjected to magnetic column-based fractionation as described above for human IgG-seq and IgA-seq. Bacterial DNA extraction and 16*S* rRNA amplification, pooling, and sequencing were also performed as described above for human IgG-seq and IgA-seq.

16*S* rRNA sequence data were processed as described above for human IgA-seq and IgG-seq using Dada2, with the exception of rarefying sequences at 21,000 reads per sample. IgA and IgG scores were calculated as the log ratio of counts of each taxon in the Ig-bound microbial fraction over counts in the Ig-unbound microbial fraction. Scores were compared across groups (*T. gondii*–infected versus uninfected) using nonparametric Mann-Whitney *U* tests. To facilitate comparisons of the capacity for IgG scores versus IgA scores to identify translocating gut microbiota members in *T. gondii*–infected mice (Fig. 2), approximately equal numbers of mice were analyzed for IgA scores (eight *T. gondii*–infected and nine uninfected) and IgG scores (nine *T. gondii*–infected and six uninfected). For intramouse comparisons of antimicrobiota IgA repertoires to antimicrobiota IgG repertoires, seven *T. gondii*–infected and seven uninfected mice were profiled for both IgG-seq and IgA-seq 4 weeks after infection. Spearman correlation tests were performed on all IgG scores compared to all IgA scores within each mouse.

IgG-seq and IgA-seq on *Y. pseudotuberculosis*–infected mice

For infections with *Y. pseudotuberculosis*, a culture of *Y. pseudotuberculosis* strain IP32777 was grown overnight in 2XYT medium with 220 rotations per minute shaking at room temperature. Suspensions were washed in PBS and resuspended to a concentration of 5×10^7/ml. Mice were infected with 10^7 colony-forming units via oral gavage. Serum and stool were collected from five *Y. pseudotuberculosis*–infected mice 4 weeks after infection and seven control, uninfected mice of equivalent age, strain, and sex. IgA-seq and IgG-seq using stool and sera were performed as described above for *T. gondii*–infected mice.

Design and construction of the human SFC

Stools from 40 healthy human donors were obtained (Lee BioSolutions, Maryland Heights, MO, USA) and subjected to DNA extraction and V4 16*S* rRNA amplification, purification, and pooling as described for paired IgA-seq and IgG-seq. Pooled libraries were sequenced on the NextSeq instrument (Illumina) using the custom R2 primer: “A+GTCAGTCAGCC+GGACTACHVGGGTWT+CTAAT” with locked nucleic acid base modifications denoted by “+.” PhiX was loaded at 40% concentration. ASV tables were

generated using Dada2, and samples were rarefied to 140,000 sequences per sample. To ensure capture of IgG titers against the greatest number of human gut microbiota members, we sought to identify the combination of samples that would yield the most diverse final community as quantified by Shannon diversity. In silico modeling was performed by randomly combining 5, 10, 15, 20, 25, 30, 35, and all 40 samples 500,000 times each. Samples were concurrently assigned random proportions of the total in silico–mixed community during each permutation. Shannon diversity values were calculated for all permutations (package "vegan" in R), and the combination of 15 participants yielding the maximum Shannon diversity was then chosen. Samples were resuspended in PBS with 1% bovine serum albumin (% w/v), mixed via gentle blending using a 21-ounce food processor, filtered through sterile 40-μm filters, OD-normalized, and added at the relative proportions dictated by the in silico modeling. The resultant SFC was centrifuged at 8000 rcf for 3.5 min and resuspended in 15% glycerol in PBS at a concentration and volume to provide sufficient SFC for 96 wells per aliquot.

IgG-seq using the human SFC

An aliquot of the SFC was thawed, centrifuged, and washed with PBS with 1% bovine serum albumin (% w/v), a buffer solution used for all subsequent stain and wash steps. Human study participants for SFC-IgG-seq (IBD and healthy participants, referring to data shown in Figs. 3 to 5) provided informed consent, and plasma was collected as part of a study approved by the Cedars-Sinai Medical Center Institutional Review Board. SFC aliquots were incubated in duplicate wells of 100 μl of human participant plasma diluted to 1:300 for 30 min at 4°C. An aliquot (1/100 volume) was taken for flow cytometry–based assessment of IgG binding. Samples were then washed via centrifugation at 6000 rcf for 4 min and resuspended in 20 μl of microbeads bound to IgG. Microbeads were made by conjugating reduced recombinant protein G with N-terminal cysteine (Novus Biologicals) to amine-functionalized magnetic beads (Alpha Biobeads) using LC-SMCC [succinimidyl 4-(*N*-maleimidomethyl)cyclohexane-1-carboxy-(6-amidocaproate)] (Thermo Fisher Scientific), using the Alpha Biobeads manufacturer protocol. Plasma-treated SFC aliquots resuspended with protein G microbeads were then shaken at 400 rpm for 20 min at room temperature. Samples were then placed on a 96-well plate magnet (Permagen, #MSP750) and allowed to bind for 2 min at room temperature. Unbound suspension (30 μl; IgG-unbound, "negative fraction") was removed from these plates, and a fixed quantity (5×10^6 colony-forming units) of *Staphylococcus hominis*, a human skin bacterium that was not present in the SFC, was added to each well to facilitate absolute quantification of taxa in the negative fraction. The suspension was frozen for downstream 16*S* rRNA amplification and sequencing on the NextSeq instrument (Illumina) as described above. A 1-μl aliquot was taken from these negative fractions for a flow cytometry–based quality check, in which cells were stained with anti-IgG PE (1:50 dilution; Miltenyi, #130093193) and SYTO-62 (1:500 dilution; Invitrogen) for 20 min at 4°C in a total volume of 50 μl, along with the pre-enrichment and post-serum incubation aliquots taken at the start of the procedure. Samples were washed, fixed in 2% PFA for 15 min at 4°C, and acquired on a Fortessa cytometer (Beckton-Dickinson) with side-scatter thresholds set to 200.

SFC-IgG-seq analysis

Sequences were processed using Dada2 (82) as above. ASVs with a total read abundance of less than 0.001% were removed. Samples were rarefied at 400,000 reads per sample using the R package "phyloseq." On a per-sample basis, all ASV counts were divided by the counts of the *S. hominis* control bacterium added for absolute quantification purposes (noted above). ASV abundances were then given a pseudo-count of the minimum nonzero value in the resulting matrix, and values were subsequently $\log_2$-transformed. IgG scores were calculated as log ratios of taxon abundances in the pre-enrichment SFC over their abundance in the IgG-unbound negative fraction. The pre-enrichment SFC consisted of 4 wells per 96-well plate that received no plasma/serum and were treated equivalently to remaining wells downstream of plasma/serum incubation. Given that these wells will have had no IgG-mediated depletion of bacteria, we name these as "pre-enrichment SFC" samples. ASV abundances in quadruplicate wells of the pre-enrichment SFC were averaged, and ASV abundances in each sample were subtracted from the averaged quadruplicate pre-enrichment SFC ASV abundances. All resulting IgG scores were averaged across sample duplicates.

Bacterial taxa were determined to be bona fide translocators if they were cultured from the mesenteric adipose tissue of more than four human participants in our cohort and if an ASV with 100% identity at the 16*S* V4 rRNA region to the same bacterium by BLAST was detected in gut mucosal microbiomes of the cohort, as obtained and sequenced by Ha *et al.* (42). This dataset has been previously deposited in BioProject: PRJNA659515. 16*S* rRNA amplicon sequence data from this dataset were processed via Dada2, and each participant's mucosal samples (involved and uninvolved mucosal biopsy sequencing samples) were aggregated by summation for the purpose of detecting the presence or absence of translocator bacteria at the gut mucosa. Samples with fewer than 19,000 total reads were excluded from analysis. ASVs in the SFC that corresponded to translocating bacterial species were identified as those having >99% identity to the translocator bacterial species (and the ASV with highest percent identity was selected in the case of multiple ASVs satisfying the stated criteria). IgG scores for those taxa were compared between healthy control participants (who did not undergo mesenteric adipose tissue sampling and culture), IBD translocation-positive participants (those for whom that bacterium was cultured from the mesenteric adipose tissue), and IBD translocation-negative participants (who underwent mesenteric adipose tissue sampling but that bacterium was not cultured from their mesenteric samples). Linear regression was performed using the aforementioned categories as ordinal variables in the presented order, with each translocator bacterium included as a random effect, comparing all translocator taxon IgG scores across the three ordinal participant categories (Fig. 3C). Taxon IgG scores were converted to z scores (centered and scaled across all participants on a per-translocator basis) and averaged within each participant category (healthy, IBD translocation-positive, and IBD translocation-negative) as inputs into the linear mixed effects model. IBD translocation-positive and IBD translocation-negative participants together consisted of 18 participants with CD and 11 participants with UD ($n = 29$ total), whereas healthy, non-IBD participants that did not undergo mesenteric sampling were $n = 9$.

Comparisons of IgG scores between IBD participant groups (e.g., healthy, CD, and UC) were performed using nonparametric statistical tests in the base "stats" library in R. For two-group comparisons, Mann-Whitney *U* tests were used ("wilcox.test"), and for three-group comparisons, the Kruskal-Wallis test was used ("kruskal. test"). For these analyses, ASVs that had nonzero count values in more than 70% of samples were examined (1071 ASVs in total). Data were visualized using the package "superheat" in R.

For visualization and comparison of total antimicrobiota IgG repertoires, an *n*-by-*n* matrix of pairwise comparisons was constructed using Pearson correlation coefficients comparing all IgG scores per sample to those of every other sample individually. Significance of group clustering was assessed using the resulting pairwise Pearson correlation matrices and the PERMANOVA technique ("adonis" function from package vegan) in R. Data were visualized using principal coordinate analyses also performed in R ("pco" from package "labdsv").

Bacterial activity and growth rate in external validation datasets

Raw shotgun metagenomics reads from the Mayo Clinic study (58) were obtained from Sequence Read Archive (BioProject accession: PRJNA487636) and processed using MetaPhlAn2 (83) to generate taxonomic relative abundance tables and Growth Rate InDex (GRiD) (56) for quantification of PTR. Reads from the METAgenomics of the Human Intestinal Tract (MetaHIT) study (57) were obtained from the European Nucleotide Archive (ENA) database (accession: PRJEB1220) and processed for PTR ratios using GRiD and using curatedMetagenomicData (84) to derive taxonomic relative abundances. The iHMP study data were obtained from tables S15 and S18 of the original publication (53). The continuous variable of dysbiosis was defined in the iHMP study in detail in the original publication. Briefly, dysbiosis scores were calculated for each individual as Bray-Curtis similarities to all healthy participant gut microbiota profiles, with higher scores denoting a greater deviation in microbiota community composition of healthy participants. All taxonomic relative abundance and GRiD values were compared between participants with CD and healthy controls for the Mayo Clinic and MetaHIT studies using nonparametric Mann-Whitney *U* tests.

To minimize the effects of microbiota-associated confounding variables (1), CD and healthy sample populations were matched for body mass index (BMI), age, and sex, where data were available. For the MetaHIT study by Nielsen *et al.*, the "healthy" participant group was chosen because this group was matched for age and sex to the CD group (age, $P = 0.93$ by two-sided *t* test; sex, $P = 0.62$ by χ^2 test), whereas the "healthy relatives" group was not matched for age ($P = 3.9 \times 10^{-5}$ by two-sided *t* test) to the CD group. This yielded a study population of 13 participants with CD and 10 healthy control participants. For the Mayo Clinic study by Muñiz Pedrogo *et al.*, individuals with rheumatoid arthritis or arthropathy were excluded from both the CD group and healthy control groups. Inclusion criteria were imposed to ensure matching for age (>25 years old) and BMI (<40 and >20 BMI), which yielded a well-matched study population for age ($P = 0.54$ by two-sided *t* test), sex ($P = 0.56$ by χ^2 test), and BMI ($P = 0.42$ by two-sided *t* test) of $N = 63$ controls and $N = 32$ participants with CD.

To facilitate comparisons to our IBD IgG-seq and translocator bacteria dataset, analyses of relative abundances and bacterial growth rate were limited to taxa classified at the species level in the metagenomics datasets. Taxa were considered translocators if they were cultured from the mesenteric adipose tissue of >4 participants in the study by Ha *et al.* (42). Taxa were considered as having significantly higher IgG scores in participants with CD if they passed the following criteria: (i) unadjusted $P < 0.05$ in Mann-Whitney U tests comparing CD to healthy participants; (ii) unadjusted $P < 0.02$ in Kruskal-Wallis tests comparing CD, UC, and healthy participants as in the analyses of Fig. 4; (iii) greater mean IgG score in CD compared to healthy participants; and (iv) >99% v4 16S rRNA sequence identity to its nearest species classification by BLAST.

Statistics

Comparisons of IgG scores to relative abundances and IgA scores to relative abundances in healthy humans with paired serum and stool samples were performed using Spearman correlation tests (R package Hmisc). IgG and IgA scores for all ASVs were compared between *T. gondii*–infected and uninfected mice using Mann-Whitney U tests ("exactRankTests" package in R). IgG scores derived from SFC-IgG-seq for translocator taxa were converted to z scores by centering and scaling, before being averaged across the three human groups: healthy control individuals, bacteria translocation–positive patients with IBD, and bacteria translocation–negative patients with IBD. Linear regression was performed for each translocating bacterial taxon included as a random effect, comparing all translocator taxon IgG scores across the three ordinal subject categories. Taxa with significant differential IgG scores between healthy, CD, and UC participants were identified using Kruskal-Wallis tests (kruskal.test in R), and taxa that differed in CD versus healthy or UC versus healthy were identified using Mann-Whitney U tests as above. Comparisons of PTR and relative abundances between patients with CD and healthy participants in both the MetaHIT and Mayo Clinic studies (Fig. 5) were performed using Mann-Whitney U tests. For all boxplots, center bars denote median and whiskers denote 1.5 * interquartile ranges.

Supplementary Material

Refer to Web version on PubMed Central for supplementary material.

Acknowledgments:

We thank A. Stacey (NIH/NIAID), N. Modi (NIH/NIAID), S.-J. Han (NIH/NIAID), S. Sen (NIH/NCI), K. Webber (NIH/NIAID), and S. C. Lee (NIH/NIAID) for assistance and helpful discussions. We thank M. Grigg (NIAID/NIH) for sharing an RFP-encoding *T. gondii* strain.

Funding:

This study was funded by the NIAID (1ZIAAI001115-11 to Y.B.), the NIH Director's Challenge Innovation Award Program (to Y.B.), the Cancer Research Institute Irvington Postdoctoral Fellowship (to I.V.-C.), the NIH Intramural AIDS Research Fellowship (to I.V.-C.), the Crohn's & Colitis Foundation Career Development Award (to I.V.-C.), and the National Cancer Institute Center for Cancer Research (1ZIABC011153-11 to G.T.). We thank the CEPHIA and its funding sources, including the Bill and Melinda Gates Foundation (OPP1017716, OPP1062806, and OPP1115799); the NIH (P01 AI071713, R01 HD074511, P30 AI027763, R24 AI067039, U01 AI043638, P01 AI074621, and R24 AI106039); the HIV Prevention Trials Network (HPTN) sponsored by the NIAID, National Institutes of Child Health and Human Development (NICH/HD), National Institute on Drug Abuse, National Institute of Mental Health, and Office of AIDS Research of the NIH, DHHS (UM1 AI068613 and R01 AI095068); the California HIV-1 Research Program (RN07-SD-702); the Brazilian Program for STD and AIDS, Ministry of

Health (914/BRA/3014-UNESCO); and the São Paulo City Health Department (2004-0.168.922-7). We also thank the Cedars-Sinai Medical Center MIRIAD Biobank for sera from IBD and non-IBD participants. Servier Medical Art (smart.servier.com) is licensed under a Creative Commons Attribution 3.0 unported license. The content of this publication does not necessarily reflect the views or policies of DHHS, nor does the mention of trade names, commercial products, or organizations imply endorsement by the U.S. government.

Data and materials availability:

Murine IgG-seq and IgA-seq data and 16*S* rRNA data may be found at NCBI under accession number PRJNA802856. Human IgA-seq and IgG-seq data on paired serum and stool samples from healthy individuals can be found at NCBI under accession number PRJNA820053. Human IgG-seq data from serum samples from patients with or without IBD using the human SFC can be found at NCBI under accession number PRJNA820056. R code for core analyses can be found at DOI: 10.5281/zenodo.6934190. All data associated with this study are present in the paper or the Supplementary Materials.

REFERENCES AND NOTES

1. Vujkovic-Cvijin I, Sklar J, Jiang L, Natarajan L, Knight R, Belkaid Y, Host variables confound gut microbiota studies of human disease. Nature 587, 448–454 (2020). [PubMed: 33149306]
2. Hausmann B, Knorr KH, Schreck K, Tringe SG, Glavina Del Rio T, Loy A, Pester M, Consortia of low-abundance bacteria drive sulfate reduction-dependent degradation of fermentation products in peat soil microcosms. ISME J. 10, 2365–2375 (2016). [PubMed: 27015005]
3. Ze X, Duncan SH, Louis P, Flint HJ, Ruminococcus bromii is a keystone species for the degradation of resistant starch in the human colon. ISME J. 6, 1535–1543 (2012). [PubMed: 22343308]
4. Thomas AM, Segata N, Multiple levels of the unknown in microbiome research. BMC Biol. 17, 48 (2019). [PubMed: 31189463]
5. Almeida A, Nayfach S, Boland M, Strozzi F, Beracochea M, Shi ZJ, Pollard KS, Sakharova E, Parks DH, Hugenholtz P, Segata N, Kyrpides NC, Finn RD, A unified catalog of 204,938 reference genomes from the human gut microbiome. Nat. Biotechnol. 39, 105–114 (2021). [PubMed: 32690973]
6. Ni J, Wu GD, Albenberg L, Tomov VT, Gut microbiota and IBD: Causation or correlation? Nat. Rev. Gastroenterol. Hepatol 14, 573–584 (2017). [PubMed: 28743984]
7. Hand TW, Vujkovic-Cvijin I, Ridaura VK, Belkaid Y, Linking the microbiota, chronic disease, and the immune system. Trends Endocrinol. Metab. 27, 831–843 (2016). [PubMed: 27623245]
8. Thaiss CA, Levy M, Grosheva I, Zheng D, Soffer E, Blacher E, Braverman S, Tengeler AC, Barak O, Elazar M, Ben-Zeev R, Lehavi-Regev D, Katz MN, Pevsner-Fischer M, Gertler A, Halpern Z, Harmelin A, Aamar S, Serradas P, Grosfeld A, Shapiro H, Geiger B, Elinav E, Hyperglycemia drives intestinal barrier dysfunction and risk for enteric infection. Science 359, 1376–1383 (2018). [PubMed: 29519916]
9. Roy S, Trinchieri G, Microbiota: A key orchestrator of cancer therapy. Nat. Rev. Cancer 17, 271–285 (2017). [PubMed: 28303904]
10. Vétizou M, Pitt JM, Daillère R, Lepage P, Waldschmitt N, Flament C, Rusakiewicz S, Routy B, Roberti MP, Duong CPM, Poirier-Colame V, Roux A, Becharef S, Formenti S, Golden E, Cording S, Eberl G, Schlitzer A, Ginhoux F, Mani S, Yamazaki T, Jacquelot N, Enot DP, Bérard M, Nigou J, Opolon P, Eggermont A, Woerther P-L, Chachaty E, Chaput N, Robert C, Mateus C, Kroemer G, Raoult D, Boneca IG, Carbonnel F, Chamaillard M, Zitvogel L, Anticancer immunotherapy by CTLA-4 blockade relies on the gut microbiota. Science 350, 1079–1084 (2015). [PubMed: 26541610]
11. Sivan A, Corrales L, Hubert N, Williams JB, Aquino-Michaels K, Earley ZM, Benyamin FW, Lei YM, Jabri B, Alegre M-L, Chang EB, Gajewski TF, Commensal Bifidobacterium promotes antitumor immunity and facilitates anti-PD-L1 efficacy. Science 350, 1084–1089 (2015). [PubMed: 26541606]

12. Geller LT, Barzily-Rokni M, Danino T, Jonas OH, Shental N, Nejman D, Gavert N, Zwang Y, Cooper ZA, Shee K, Thaiss CA, Reuben A, Livny J, Avraham R, Frederick DT, Ligorio M, Chatman K, Johnston SE, Mosher CM, Brandis A, Fuks G, Gurbatri C, Gopalakrishnan V, Kim M, Hurd MW, Katz M, Fleming J, Maitra A, Smith DA, Skalak M, Bu J, Michaud M, Trauger SA, Barshack I, Golan T, Sandbank J, Flaherty KT, Mandinova A, Garrett WS, Thayer SP, Ferrone CR, Huttenhower C, Bhatia SN, Gevers D, Wargo JA, Golub TR, Straussman R, Potential role of intratumor bacteria in mediating tumor resistance to the chemotherapeutic drug gemcitabine. Science 357, 1156–1160 (2017). [PubMed: 28912244]
13. Iida N, Dzutsev A, Stewart CA, Smith L, Bouladoux N, Weingarten RA, Molina DA, Salcedo R, Back T, Cramer S, Dai R-M, Kiu H, Cardone M, Naik S, Patri AK, Wang E, Marincola FM, Frank KM, Belkaid Y, Trinchieri G, Goldszmid RS, Commensal bacteria control cancer response to therapy by modulating the tumor microenvironment. Science 342, 967–970 (2013). [PubMed: 24264989]
14. Poore GD, Kopylova E, Zhu Q, Carpenter C, Fraraccio S, Wandro S, Kosciolek T, Janssen S, Metcalf J, Song SJ, Kanbar J, Miller-Montgomery S, Heaton R, Mckay R, Patel SP, Swafford AD, Knight R, Microbiome analyses of blood and tissues suggest cancer diagnostic approach. Nature 579, 567–574 (2020). [PubMed: 32214244]
15. de Goffau MC, Lager S, Sovio U, Gaccioli F, Cook E, Peacock SJ, Parkhill J, Charnock-Jones DS, Smith GCS, Human placenta has no microbiome but can contain potential pathogens. Nature 572, 329–334 (2019). [PubMed: 31367035]
16. Kau AL, Planer JD, Liu J, Rao S, Yatsunenko T, Trehan I, Manary MJ, Liu T-C, Stappenbeck TS, Maleta KM, Ashorn P, Dewey KG, Houpt ER, Hsieh C-S, Gordon JI, Functional characterization of IgA-targeted bacterial taxa from undernourished Malawian children that produce diet-dependent enteropathy. Sci. Transl. Med. 7, 276ra24 (2015).
17. Palm NW, De Zoete MR, Cullen TW, Barry NA, Stefanowski J, Hao L, Degnan PH, Hu J, Peter I, Zhang W, Ruggiero E, Cho JH, Goodman AL, Flavell RA, Immunoglobulin A coating identifies colitogenic bacteria in inflammatory bowel disease. Cell 158, 1000–1010 (2014). [PubMed: 25171403]
18. Bunker JJ, Flynn TM, Koval JC, Shaw DG, Meisel M, McDonald BD, Ishizuka IE, Dent AL, Wilson PC, Jabri B, Antonopoulos DA, Bendelac A, Innate and adaptive humoral responses coat distinct commensal bacteria with immunoglobulin A. Immunity 43, 541–553 (2015). [PubMed: 26320660]
19. Koch MA, Reiner GL, Lugo KA, Kreuk LSM, Stanbery AG, Ansaldo E, Seher TD, Ludington WB, Barton GM, Maternal IgG and IgA antibodies dampen mucosal t helper cell responses in early life. Cell 165, 827–841 (2016). [PubMed: 27153495]
20. Viladomiu M, Kivolowitz C, Abdulhamid A, Dogan B, Victorio D, Castellanos JG, Woo V, Teng F, Tran NL, Sczesnak A, Chai C, Kim M, Diehl GE, Ajami NJ, Petrosino JF, Zhou XK, Schwartzman S, Mandl LA, Abramowitz M, Jacob V, Bosworth B, Steinlauf A, Scherl EJ, Wu HJJ, Simpson KW, Longman RS, IgA-coated E *coli* enriched in Crohn's disease spondyloarthritis promote T_H17-dependent inflammation. Sci. Transl. Med. 9, eaaf9655 (2017). [PubMed: 28179509]
21. Chen K, Magri G, Grasset EK, Cerutti A, Rethinking mucosal antibody responses: IgM, IgG and IgD join IgA. Nat. Rev. Immunol. 20, 427–441 (2020). [PubMed: 32015473]
22. Phalipon A, Cardona A, Kraehenbuhl JP, Edelman L, Sansonetti PJ, Corthésy B, Secretory component: A new role in secretory IgA-mediated immune exclusion in vivo. Immunity 17, 107–115 (2002). [PubMed: 12150896]
23. Donaldson GP, Ladinsky MS, Yu KB, Sanders JG, Yoo BB, Chou WC, Conner ME, Earl AM, Knight R, Bjorkman PJ, Mazmanian SK, Gut microbiota utilize immunoglobulin a for mucosal colonization. Science 360, 795–800 (2018). [PubMed: 29724905]
24. Petersen C, Bell R, Klag KA, Lee SH, Soto R, Ghazaryan A, Buhrke K, Atakan Ekiz H, Ost KS, Boudina S, O'Connell RM, Cox JE, Villanueva CJ, Zac Stephens W, Round JL, T cell–mediated regulation of the microbiota protects against obesity. Science 635, eaat9351 (2019).
25. Ansaldo E, Farley TK, Belkaid Y, Control of immunity by the microbiota. Annu. Rev. Immunol. 39, 449–479 (2021). [PubMed: 33902310]
26. Elson CO, Ealding W, Generalized systemic and mucosal immunity in mice after mucosal stimulation with cholera toxin. J. Immunol. 132, 2736–2741 (1984). [PubMed: 6233359]

27. Li H, Limenitakis JP, Greiff V, Yilmaz B, Schären O, Urbaniak C, Zünd M, Lawson MAE, Young ID, Rupp S, Heikenwälder M, McCoy KD, Hapfelmeier S, Ganal-Vonarburg SC, Macpherson AJ, Mucosal or systemic microbiota exposures shape the B cell repertoire. Nature 584, 274–278 (2020). [PubMed: 32760003]
28. Geiger SM, Massara CL, Bethony J, Soboslay PT, Carvalho OS, Corrêa-Oliveira R, Cellular responses and cytokine profiles in Ascaris lumbricoides and Trichuris trichiura infected patients. Parasite Immunol. 24, 499–509 (2002). [PubMed: 12694600]
29. Bernin H, Marggraff C, Jacobs T, Brattig N, Van An L, Blessmann J, Lotter H, Immune markers characteristic for asymptomatically infected and diseased Entamoeba histolytica individuals and their relation to sex. BMC Infect. Dis. 14, 621 (2014). [PubMed: 25420932]
30. Vazquez-Torres A, Jones-Carson J, Bäumler AJ, Falkow S, Valdivia R, Brown W, Le M, Berggren R, Parks WT, Fang FC, Extraintestinal dissemination of *Salmonella* by CD18-expressing phagocytes. Nature 401, 804–808 (1999). [PubMed: 10548107]
31. Peter Rissing J, Buxton TB, Edmondson HT, Detection of specific IgG antibody in sera from patients infected with *Bacteroides fragilis* by enzyme-linked immunosorbent assay. J Infect Dis 140, 994–998 (1979). [PubMed: 396340]
32. Zeng MY, Cisalpino D, Varadarajan S, Hellman J, Warren HS, Cascalho M, Inohara N, Núñez G, Gut microbiota-induced immunoglobulin G controls systemic infection by symbiotic bacteria and pathogens. Immunity 44, 647–658 (2016). [PubMed: 26944199]
33. Ansaldo E, Slayden LC, Ching KL, Koch MA, Wolf NK, Plichta DR, Brown EM, Graham DB, Xavier RJ, Moon JJ, Barton GM, *Akkermansia muciniphila* induces intestinal adaptive immune responses during homeostasis. Science 364, 1179–1184 (2019). [PubMed: 31221858]
34. Fadlallah J, Sterlin D, Fieschi C, Parizot C, Dorgham K, El Kafsi H, Autaa G, Ghillani-Dalbin P, Juste C, Lepage P, Malphettes M, Galicier L, Boutboul D, Clément K, André S, Marquet F, Tresallet C, Mathian A, Miyara M, Oksenhendler E, Amoura Z, Yssel H, Larsen M, Gorochov G, Synergistic convergence of microbiota-specific systemic IgG and secretory IgA. J. Allergy Clin. Immunol. 143, 1575–1585.e4 (2019). [PubMed: 30554723]
35. Barragan A, Sibley LD, Migration of Toxoplasma gondii across biological barriers. Trends Microbiol. 11, 426–430 (2003). [PubMed: 13678858]
36. Hand TW, Dos Santos LM, Bouladoux N, Molloy MJ, Pagán AJ, Pepper M, Maynard CL, Elson CO, Belkaid Y, Acute gastrointestinal infection induces long-lived microbiota-specific T cell responses. Science 337, 1553–1556 (2012). [PubMed: 22923434]
37. Da Fonseca DM, Hand TW, Han SJ, Gerner MY, Zaretsky AG, Byrd AL, Harrison OJ, Ortiz AM, Quinones M, Trinchieri G, Brenchley JM, Brodsky IE, Germain RN, Randolph GJ, Belkaid Y, Microbiota-dependent sequelae of acute infection compromise tissue-specific immunity. Cell 163, 354–366 (2015). [PubMed: 26451485]
38. McKenna P, Hoffmann C, Minkah N, Aye PP, Lackner A, Liu Z, Lozupone CA, Hamady M, Knight R, Bushman FD, The macaque gut microbiome in health, lentiviral infection, and chronic enterocolitis. PLOS Pathog. 4, e20 (2008). [PubMed: 18248093]
39. Salzman NH, Hung K, Haribhai D, Chu H, Karlsson-Sjöberg J, Amir E, Teggatz P, Barman M, Hayward M, Eastwood D, Stoel M, Zhou Y, Sodergren E, Weinstock GM, Bevins CL, Williams CB, Bos NA, Enteric defensins are essential regulators of intestinal microbial ecology. Nat. Immunol. 11, 76–83 (2010). [PubMed: 19855381]
40. Moor K, Fadlallah J, Toska A, Sterlin D, Balmer ML, Macpherson AJ, Gorochov G, Larsen M, Slack E, Analysis of bacterial-surface-specific antibodies in body fluids using bacterial flow cytometry. Nat. Protoc. 11, 1531–1553 (2016). [PubMed: 27466712]
41. Rollenske T, Burkhalter S, Muerner L, von Gunten S, Lukasiewicz J, Wardemann H, Macpherson AJ, Parallelism of intestinal secretory IgA shapes functional microbial fitness. Nature 598, 657–661 (2021). [PubMed: 34646015]
42. Ha CWY, Martin A, Sepich-Poore GD, Shi B, Wang Y, Gouin K, Humphrey G, Sanders K, Ratnayake Y, Chan KSL, Hendrick G, Caldera JR, Arias C, Moskowitz JE, Ho Sui SJ, Yang S, Underhill D, Brady MJ, Knott S, Kaihara K, Steinbaugh MJ, Li H, McGovern DPB, Knight R, Fleshner P, Devkota S, Translocation of viable gut microbiota to mesenteric adipose drives formation of creeping fat in humans. Cell 183, 666–683.e17 (2020). [PubMed: 32991841]

43. Van Der Waaij LA, Kroese FGM, Visser A, Nelis GF, Westerveld BD, Jansen PLM, Hunter JO, Immunoglobulin coating of faecal bacteria in inflammatory bowel disease. Eur. J. Gastroenterol. Hepatol. 16, 669–674 (2004). [PubMed: 15201580]
44. Furrie E, Macfarlane S, Cummings JH, Macfarlane GT, Systemic antibodies towards mucosal bacteria in ulcerative colitis and Crohn's disease differentially activate the innate immune response. Gut 53, 91–98 (2004). [PubMed: 14684582]
45. Adams RJ, Heazlewood SP, Gilshenan KS, O'Brien M, McGuckin MA, Florin THJ, IgG antibodies against common gut bacteria are more diagnostic for Crohn's disease than IgG against mannan or flagellin. Am. J. Gastroenterol. 103, 386–396 (2008). [PubMed: 17924999]
46. Macpherson A, Khoo UY, Forgacs I, Philpott-Howard J, Bjarnason I, Mucosal antibodies in inflammatory bowel disease are directed against intestinal bacteria. Gut 38, 365–375 (1996). [PubMed: 8675088]
47. Harmsen HJM, Pouwels SD, Funke A, Bos NA, Dijkstra G, Crohn's disease patients have more IgG-binding fecal bacteria than controls. Clin. Vaccine Immunol. 19, 515–521 (2012). [PubMed: 22336288]
48. Rengarajan S, Vivio EE, Parkes M, Peterson DA, Roberson EDO, Newberry RD, Ciorba MA, Hsieh CS, Dynamic immunoglobulin responses to gut bacteria during inflammatory bowel disease. Gut Microbes 11, 405–420 (2020). [PubMed: 31203722]
49. Castro-Dopico T, Dennison TW, Ferdinand JR, Mathews RJ, Fleming A, Clift D, Stewart BJ, Jing C, Strongili K, Labzin LI, Monk EJM, Saeb-Parsy K, Bryant CE, Clare S, Parkes M, Clatworthy MR, Anti-commensal IgG drives intestinal inflammation and type 17 immunity in ulcerative colitis. Immunity 50, 1099–1114.e10 (2019). [PubMed: 30876876]
50. Flyak AI, Shen X, Murin CD, Turner HL, David JA, Fusco ML, Lampley R, Kose N, Ilinykh PA, Kuzmina N, Branchizio A, King H, Brown L, Bryan C, Davidson E, Doranz BJ, Slaughter JC, Sapparapu G, Klages C, Ksiazek TG, Saphire EO, Ward AB, Bukreyev A, Crowe JE Jr., Cross-reactive and potent neutralizing antibody responses in human survivors of natural ebolavirus infection. Cell 164, 392–405 (2016). [PubMed: 26806128]
51. Nachbagauer R, Choi A, Hirsh A, Margine I, Iida S, Barrera A, Ferres M, Albrecht RA, García-Sastre A, Bouvier NM, Ito K, Medina RA, Palese P, Krammer F, Defining the antibody cross-reactome directed against the influenza virus surface glycoproteins. Nat. Immunol. 18, 464–473 (2017). [PubMed: 28192418]
52. Korem T, Zeevi D, Suez J, Weinberger A, Avnit-Sagi T, Pompan-Lotan M, Matot E, Jona G, Harmelin A, Cohen N, Sirota-Madi A, Thaiss CA, Pevsner-Fischer M, Sorek R, Xavier RJ, Elinav E, Segal E, Growth dynamics of gut microbiota in health and disease inferred from single metagenomic samples. Science 349, 1101–1106 (2015). [PubMed: 26229116]
53. Lloyd-Price J, Arze C, Ananthakrishnan AN, Schirmer M, Avila-Pacheco J, Poon TW, Andrews E, Ajami NJ, Bonham KS, Brislawn CJ, Casero D, Courtney H, Gonzalez A, Graeber TG, Hall AB, Lake K, Landers CJ, Mallick H, Plichta DR, Prasad M, Rahnavard G, Sauk J, Shungin D, Vázquez-Baeza Y, White RA, Braun J, Denson LA, Jansson JK, Knight R, Kugathasan S, McGovern DPB, Petrosino JF, Stappenbeck TS, Winter HS, Clish CB, Franzosa EA, Vlamakis H, Xavier RJ, Huttenhower C, Multi-omics of the gut microbial ecosystem in inflammatory bowel diseases. Nature, 655–662 (2019).
54. Blazewicz SJ, Barnard RL, Daly RA, Firestone MK, Evaluating rRNA as an indicator of microbial activity in environmental communities: Limitations and uses. ISME J. 7, 2061–2068 (2013). [PubMed: 23823491]
55. Klumpp S, Zhang Z, Hwa T, Growth rate-dependent global effects on gene expression in bacteria. Cell 139, 1366–1375 (2009). [PubMed: 20064380]
56. Emiola A, Oh J, High throughput in situ metagenomic measurement of bacterial replication at ultra-low sequencing coverage. Nat. Commun. 9, 4956 (2018). [PubMed: 30470746]
57. Nielsen HB, Almeida M, Juncker AS, Rasmussen S, Li J, Sunagawa S, Plichta DR, Gautier L, Pedersen AG, Le Chatelier E, Pelletier E, Bonde I, Nielsen T, Manichanh C, Arumugam M, Batto JM, Santos MBQD, Blom N, Borruel N, Burgdorf KS, Boumezbeur F, Casellas F, Doré J, Dworzynski P, Guarner F, Hansen T, Hildebrand F, Kaas RS, Kennedy S, Kristiansen K, Kultima JR, Leonard P, Levenez F, Lund O, Moumen B, Le Paslier D, Pons N, Pedersen O, Prifti E, Qin J, Raes J, Sørensen S, Tap J, Tims S, Ussery DW, Yamada T, Renault P, Sicheritz-Ponten T, Bork

P, Wang J, Brunak S, Ehrlich SD; MetaHIT Consortium, Identification and assembly of genomes and genetic elements in complex metagenomic samples without using reference genomes. Nat. Biotechnol. 32, 822–828 (2014). [PubMed: 24997787]

58. Muñiz Pedrogo DA, Chen J, Hillmann B, Jeraldo P, Al-Ghalith G, Taneja V, Davis JM, Knights D, Nelson H, Faubion WA, Raffals L, Kashyap PC, An increased abundance of clostridiaceae characterizes arthritis in inflammatory bowel disease and rheumatoid arthritis: A cross-sectional study. Inflamm. Bowel Dis. 25, 902–913 (2019). [PubMed: 30321331]
59. Yilmaz B, Juillerat P, Øyås O, Ramon C, Bravo FD, Franc Y, Fournier N, Michetti P, Mueller C, Geuking M, Pittet VEH, Maillard MH, Rogler G; Swiss IBD Cohort Investigators, Wiest R, Stelling J, Macpherson AJ, Microbial network disturbances in relapsing refractory Crohn's disease. Nat. Med. 25, 323–336 (2019). [PubMed: 30664783]
60. Kugathasan S, Denson LA, Walters TD, Kim MO, Marigorta UM, Schirmer M, Mondal K, Liu C, Griffiths A, Noe JD, Crandall WV, Snapper S, Rabizadeh S, Rosh JR, Shapiro JM, Guthery S, Mack DR, Kellermayer R, Kappelman MD, Steiner S, Moulton DE, Keljo D, Cohen S, Oliva-Hemker M, Heyman MB, Otley AR, Baker SS, Evans JS, Kirschner BS, Patel AS, Ziring D, Trapnell BC, Sylvester FA, Stephens MC, Baldassano RN, Markowitz JF, Cho J, Xavier RJ, Huttenhower C, Aronow BJ, Gibson G, Hyams JS, Dubinsky MC, Prediction of complicated disease course for children newly diagnosed with Crohn's disease: A multicentre inception cohort study. Lancet 389, 1710–1718 (2017). [PubMed: 28259484]
61. Geva-Zatorsky N, Sefik E, Kua L, Pasman L, Tan TG, Ortiz-Lopez A, Yanortsang TB, Yang L, Jupp R, Mathis D, Benoist C, Kasper DL, Mining the human gut microbiota for immunomodulatory organisms. Cell 168, 928–943.e11 (2017). [PubMed: 28215708]
62. Tan TG, Sefik E, Geva-Zatorsky N, Kua L, Naskar D, Teng F, Pasman L, Ortiz-Lopez A, Jupp R, Wu HJJ, Kasper DL, Benoist C, Mathis D, Identifying species of symbiont bacteria from the human gut that, alone, can induce intestinal Th17 cells in mice. Proc. Natl. Acad. Sci. U.S.A. 113, E8141–E8150 (2016). [PubMed: 27911839]
63. Moschen AR, Tilg H, Raine T, IL-12, IL-23 and IL-17 in IBD: Immunobiology and therapeutic targeting. Nat. Rev. Gastroenterol. Hepatol. 16, 185–196 (2019). [PubMed: 30478416]
64. Eken A, Singh AK, Treuting PM, Oukka M, IL-23R+ innate lymphoid cells induce colitis via interleukin-22-dependent mechanism. Mucosal Immunol. 7, 143–154 (2014). [PubMed: 23715173]
65. Falugi F, Kim HK, Missiakas DM, Schneewind O, Role of protein A in the evasion of host adaptive immune responses by Staphylococcus aureus. MBio 4, e00575 (2013). [PubMed: 23982075]
66. O'Brien CL, Pavli P, Gordon DM, Allison GE, Detection of bacterial DNA in lymph nodes of Crohn's disease patients using high throughput sequencing. Gut 63, 1596–1606 (2014). [PubMed: 24429583]
67. Kiely CJ, Pavli P, O'Brien CL, The microbiome of translocated bacterial populations in patients with and without inflammatory bowel disease. Intern. Med. J. 48, 1346–1354 (2018). [PubMed: 29893034]
68. Abreu RB, Clutter EF, Attari S, Sautto GA, Ross TM, IgA responses following recurrent influenza virus vaccination. Front. Immunol. 11, 902 (2020). [PubMed: 32508822]
69. Kang ZH, Bricault CA, Borducchi EN, Stephenson KE, Seaman MS, Pau M, Schuitemaker H, van Manen D, Wegmann F, Barouch DH, Similar epitope specificities of IgG and IgA antibodies elicited by Ad26 vector prime, env protein boost immunizations in rhesus monkeys. J. Virol. 92, e00537–18 (2018). [PubMed: 29793950]
70. Wilmore JR, Gaudette BT, GomezAtria D, Hashemi T, Jones DD, Gardner CA, Cole SD, Misic AM, Beiting DP, Allman D, Commensal microbes induce serum IgA responses that protect against polymicrobial sepsis. Cell Host Microbe 23, 302–311.e3 (2018). [PubMed: 29478774]
71. Ost KS, O'Meara TR, Stephens WZ, Chiaro T, Zhou H, Penman J, Bell R, Catanzaro JR, Song D, Singh S, Call DH, Hwang-Wong E, Hanson KE, Valentine JF, Christensen KA, O'Connell RM, Cormack B, Ibrahim AS, Palm NW, Noble SM, Round JL, Adaptive immunity induces mutualism between commensal eukaryotes. Nature 596, 114–118 (2021). [PubMed: 34262174]
72. Cullender TC, Chassaing B, Janzon A, Kumar K, Muller CE, Werner JJ, Angenent LT, Bell ME, Hay AG, Peterson DA, Walter J, Vijay-Kumar M, Gewirtz AT, Ley RE, Innate and adaptive

immunity interact to quench microbiome flagellar motility in the gut. Cell Host Microbe 14, 571–581 (2013). [PubMed: 24237702]

73. Chen L, Wilson JE, Koenigsknecht MJ, Chou WC, Montgomery SA, Truax AD, Brickey WJ, Packey CD, Maharshak N, Matsushima GK, Plevy SE, Young VB, Sartor RB, Ting JPY, NLRP12 attenuates colon inflammation by maintaining colonic microbial diversity and promoting protective commensal bacterial growth. Nat. Immunol. 18, 541–551 (2017). [PubMed: 28288099]
74. Surana NK, Kasper DL, Moving beyond microbiome-wide associations to causal microbe identification. Nature 552, 244–247 (2017). [PubMed: 29211710]
75. Vital M, Karch A, Pieper DH, Colonic butyrate-producing communities in humans: An overview using omics data. mSystems 2, e00130–17 (2017). [PubMed: 29238752]
76. Furusawa Y, Obata Y, Fukuda S, Endo TA, Nakato G, Takahashi D, Nakanishi Y, Uetake C, Kato K, Kato T, Takahashi M, Fukuda NN, Murakami S, Miyauchi E, Hino S, Atarashi K, Onawa S, Fujimura Y, Lockett T, Clarke JM, Topping DL, Tomita M, Hori S, Ohara O, Morita T, Koseki H, Kikuchi J, Honda K, Hase K, Ohno H, Commensal microbe-derived butyrate induces the differentiation of colonic regulatory T cells. Nature 504, 446–450 (2013). [PubMed: 24226770]
77. Takahashi D, Hoshina N, Kabumoto Y, Maeda Y, Suzuki A, Tanabe H, Isobe J, Yamada T, Muroi K, Yanagisawa Y, Nakamura A, Fujimura Y, Saeki A, Ueda M, Matsumoto R, Asaoka H, Clarke JM, Harada Y, Umemoto E, Komatsu N, Okada T, Takayanagi H, Takeda K, Tomura M, Hase K, Microbiota-derived butyrate limits the autoimmune response by promoting the differentiation of follicular regulatory T cells. EBioMedicine 58, 102913 (2020). [PubMed: 32711255]
78. Rollenske T, Szijarto V, Lukasiewicz J, Guachalla LM, Stojkovic K, Hartl K, Stulik L, Kocher S, Lasitschka F, Al-Saeedi M, Schröder-Braunstein J, Von Frankenberg M, Gaebelein G, Hoffmann P, Klein S, Heeg K, Nagy E, Nagy G, Wardemann H, Cross-specificity of protective human antibodies against *Klebsiella pneumoniae* LPS O-antigen. Nat. Immunol. 19, 617–624 (2018). [PubMed: 29760533]
79. Lv H, Wu NC, Tsang OTY, Yuan M, Perera RAPM, Leung WS, So RTY, Chan JMC, Yip GK, Chik TSH, Wang Y, Choi CYC, Lin Y, Ng WW, Zhao J, Poon LLM, Peiris JSM, Wilson IA, Mok CKP, Cross-reactive antibody response between SARS-CoV-2 and SARS-CoV infections. Cell Rep. 31, 107725 (2020).
80. Vogl T, Klompus S, Leviatan S, Kalka IN, Weinberger A, Wijmenga C, Fu J, Zhernakova A, Weersma RK, Segal E, Population-wide diversity and stability of serum antibody epitope repertoires against human microbiota. Nat. Med. 27, 1442–1450 (2021). [PubMed: 34282338]
81. Ji BW, Sheth RU, Dixit PD, Huang Y, Kaufman A, Wang HH, Vitkup D, Quantifying spatiotemporal variability and noise in absolute microbiota abundances using replicate sampling. Nat. Methods 16, 731–736 (2019). [PubMed: 31308552]
82. Callahan BJ, McMurdie PJ, Rosen MJ, Han AW, Johnson AJA, Holmes SP, DADA2: High-resolution sample inference from Illumina amplicon data. Nat. Methods 13, 581–583 (2016). [PubMed: 27214047]
83. Segata N, Waldron L, Ballarini A, Narasimhan V, Jousson O, Huttenhower C, Metagenomic microbial community profiling using unique clade-specific marker genes. Nat. Methods 9, 811–814 (2012). [PubMed: 22688413]
84. Pasolli E, Schiffer L, Manghi P, Renson A, Obenchain V, Truong DT, Beghini F, Malik F, Ramos M, Dowd JB, Huttenhower C, Morgan M, Segata N, Waldron L, Accessible, curated metagenomic data through ExperimentHub. Nat. Methods 14, 1023–1024 (2017). [PubMed: 29088129]

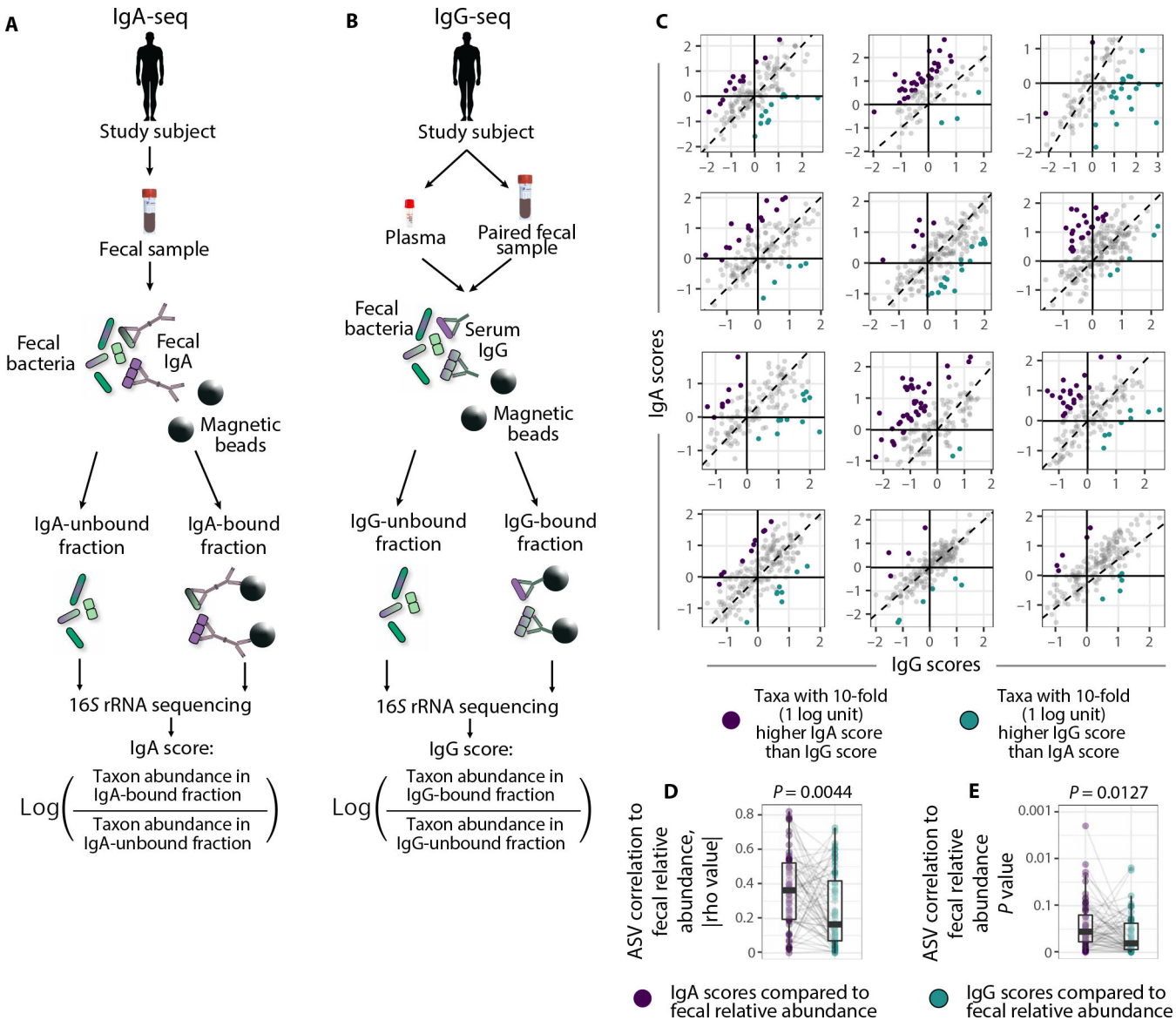

Fig. 1. Fecal IgA and systemic IgG target different gut microbiota constituents.

(A) Shown is the IgA-seq workflow. Fecal bacteria from mice and humans were incubated with phycoerythrin (PE)–conjugated anti-IgA antibodies, after which anti-PE microbeads facilitated magnetic separation of IgA-bound bacteria from IgA-unbound bacteria. These two fractions were subjected to 16S rRNA sequencing, and IgA scores for each taxon [i.e., amplicon sequence variant (ASV)] were calculated as the log ratio of taxon relative abundance in the IgA-bound fraction over that in the unbound fraction. **(B)** Shown is the IgG-seq workflow. Fecal bacteria were incubated with autologous sera and stained with PE anti-IgG antibodies, fractionated, and sequenced as for IgA-seq. (**C**) Many gut bacterial taxa in stool samples exhibited differential binding by mucosal IgA and serum IgG from healthy individuals ($n = 12$). Taxa with 10-fold higher IgA scores than IgG scores are depicted in purple, whereas taxa with 10-fold higher IgG scores are in green. (**D** and **E**) IgA scores correlated more strongly with baseline fecal relative abundances than IgG scores. (D) Shown

are absolute values of all Spearman rho values for correlations comparing IgA or IgG scores to fecal relative abundances among taxa whose IgA and IgG scores differed by 10-fold [green and purple dots in (C)]. (E) Spearman *P* values for the same comparisons as in (D). Paired ratio *t* tests were performed for (D) and on log-transformed values of (E).

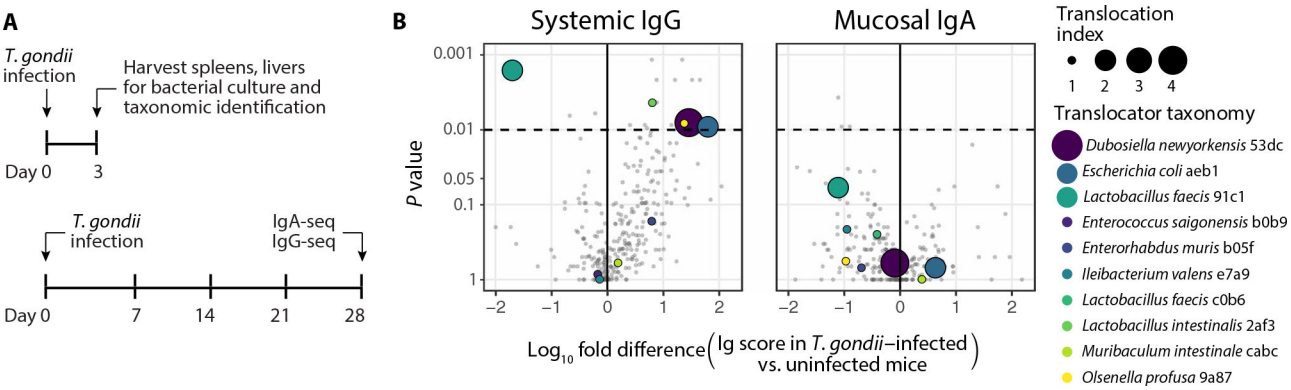

Fig. 2. Systemic IgG identifies gut bacteria capable of translocation.

(**A**) Shown is the experimental plan. Livers and spleens of acute *T. gondii*–infected mice were processed and subjected to bacterial culture at day 3 after infection. Bacterial colonies were identified using full-length 16*S* rRNA sequencing. IgA-seq and IgG-seq were performed at day 28 after infection ($n = 17$ mice for IgA-seq and $n = 15$ mice for IgG-seq, across three independent experiments). (**B**) Shown are translocating bacterial species that were cultured from mouse livers or spleens in one or more independent experiments. Translocation index refers to the number of independent experiments ($n = 4$ to 7 *T. gondii*–infected mice per experiment) in which translocating bacterial species was cultured. Mean fold differences in IgA and IgG scores between *T. gondii*–infected and uninfected mice were calculated for each taxon, and Mann-Whitney *U* tests were performed to calculate *P* values.

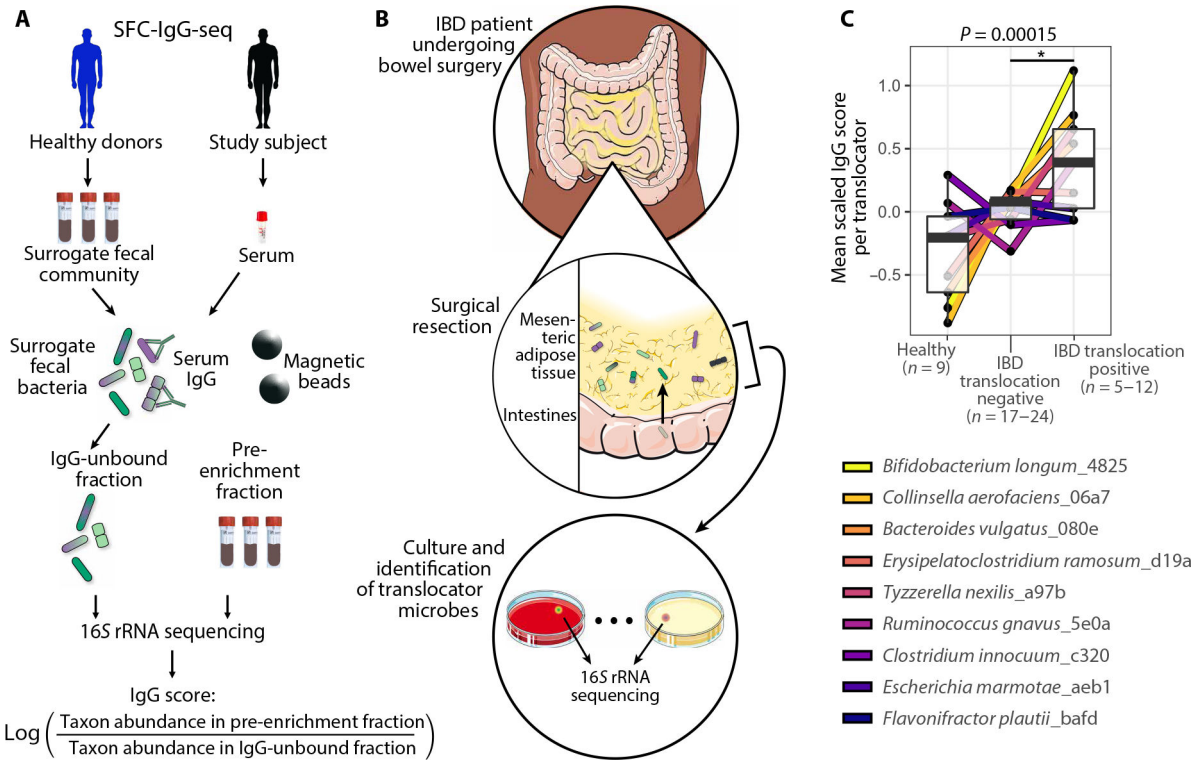

Fig. 3. Translocating bacteria exhibit heightened IgG scores in humans.

(**A**) Shown is the SFC-IgG-seq workflow. In the absence of stool samples from study participants, a surrogate fecal community (SFC) comprising a combination of healthy donor feces from a separate cohort was prepared [see fig. S3 (A and B)]. Fecal bacteria and sera were co-incubated, and the IgG-unbound fraction was sequenced along with triplicate pre-enrichment aliquots of the SFC. IgG scores were calculated, comparing taxon abundances to the pre-enrichment community (see fig. S3C). (**B**) To identify translocating bacteria in a cohort of patients with IBD undergoing medically indicated bowel resection surgery, mesenteric adipose tissue from resected small and large intestinal samples was subjected to bacterial culture. Full-length 16*S* rRNA sequencing was then performed on bacterial colonies to identify translocating bacteria for each individual. (**C**) SFC-IgG-seq was performed using serum samples from $n = 29$ patients with IBD and $n = 9$ healthy individuals. For each taxon, mean scaled IgG scores were compared across healthy individuals, patients with IBD with no detected translocation for that taxon, and patients with IBD for whom that taxon was cultured from the mesenteric adipose tissue ("translocation positive"). These groups were treated as ordinal variables in that order, and linear regression on IgG scores was performed, grouping all taxa ($P = 0.00015$). IgG scores for translocating bacterial taxa (translocator) were elevated in translocation-positive patients with IBD compared to translocation-negative patients with IBD ($P = 0.0268$, paired two-sided Student's t test). $*P < 0.05$.

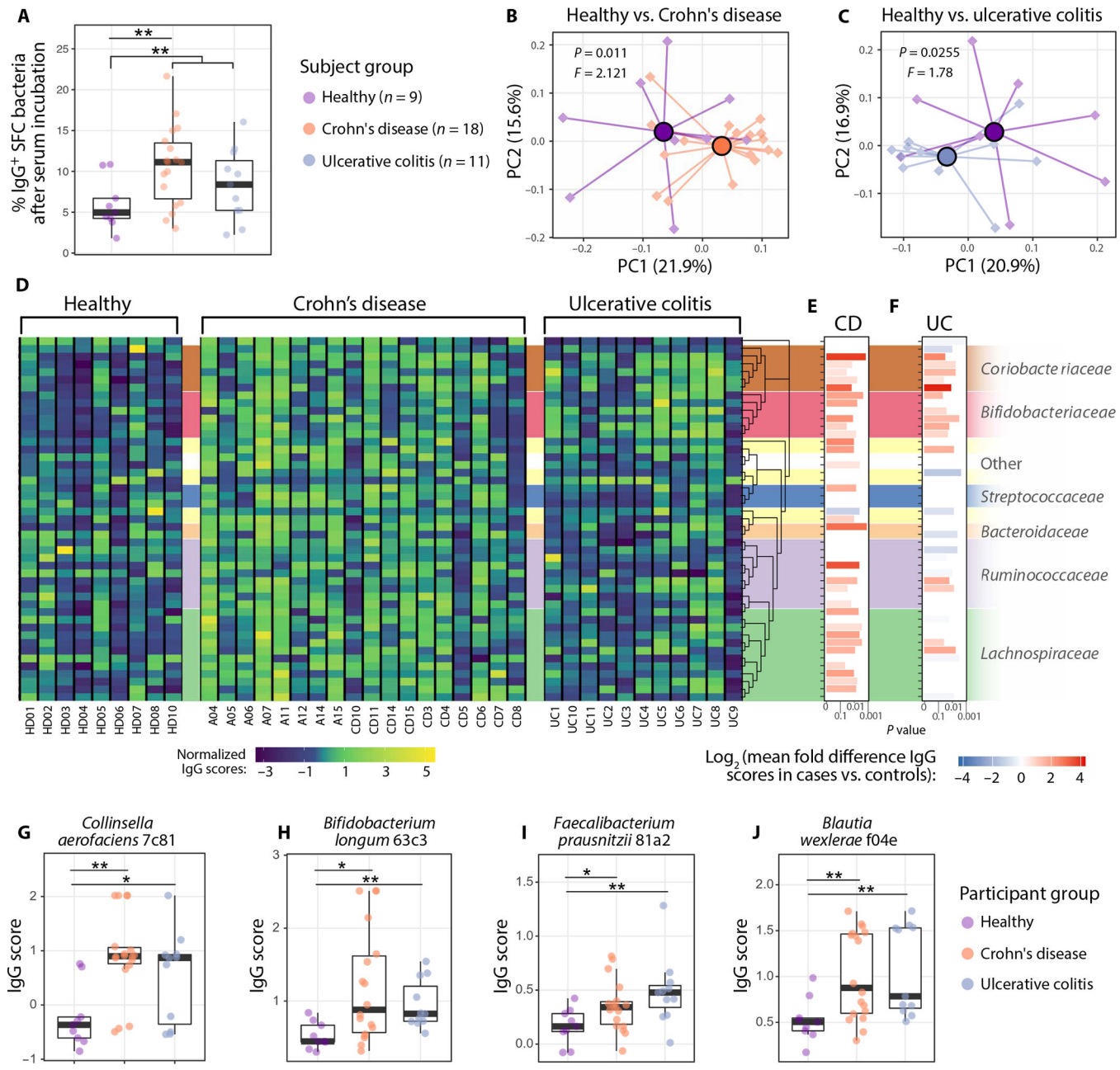

Fig. 4. Antimicrobiota IgG profiles differ between patients with IBD and healthy individuals.

(**A**) Percentages of bacteria in the SFC bound by IgG were determined for each study participant using flow cytometry [healthy versus Crohn's disease (CD), $P = 0.0053$; healthy versus IBD, $P = 0.0095$; healthy versus ulcerative colitis (UC), $P = 0.26$; two-sided Student's *t* test]. (**B** and **C**) Principal coordinates (PC) analyses using pairwise Pearson correlation coefficient matrices encompassing IgG scores for all taxa are shown. *P* values and *F* statistics were calculated using PERMANOVA. (**D**) Heatmap of all taxa whose IgG scores differed among the three groups (unadjusted $P < 0.02$, Kruskal-Wallis test). (**E** and **F**) Shown are taxa whose IgG scores differed significantly between (E) healthy individuals and patients with CD and (F) healthy individuals and patients with UC ($P < 0.05$, Mann-Whitney

U test). (**G** to **J**) Shown are plots depicting IgG scores of representative members of genera that differed in IgG scores between healthy individuals and patients with IBD. Shown are IgG scores for *Collinsella aerofaciens* (G), *Bifidobacterium longum* (H), *Faecalibacterium prausnitzii* (I), and *Blautia wexlerae* (J). $^{**}P < 0.01$ and $^{*}P < 0.05$; Mann-Whitney *U* test.

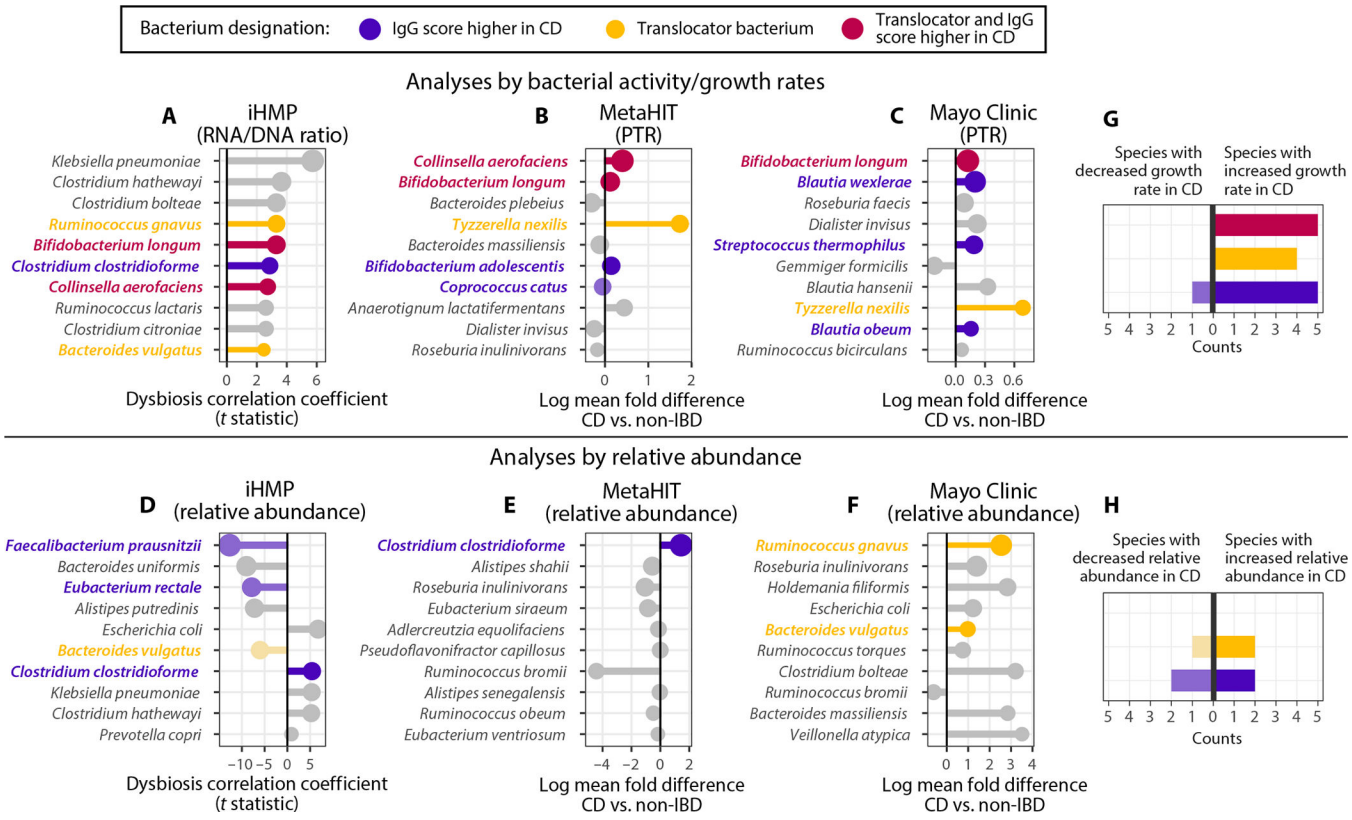

Fig. 5. Bacterial growth correlates more strongly with translocator status and IgG score dynamics than does relative abundance in CD.

(**A** to **F**) Analyses of external, independent metagenomics datasets of patients with CD and healthy individuals, using markers of bacterial growth (A to C) and relative abundance (D to F). Bacterial species were ranked by resulting *P* values and are shown in order, with the most significant at the top of each graph. The top 10 taxa classified at the species level for each analysis are shown with *P* values in table S6. Bacteria of the following categories are highlighted in color: those with higher IgG scores in CD (defined in Materials and Methods), those that were cultured from ≥5 mesenteric adipose tissue samples in our IBD cohort, and those that were both cultured from mesenteric adipose tissue and exhibited heightened IgG scores in CD. (A) RNA/DNA ratios for each bacterium, a proxy for bacterial cell growth, were compared [as described previously (53)] to a marker of longitudinal gut dysbiosis for patients with CD ($n = 106$), and the resulting strength of correlation is shown on the *x* axis. (B and C) Peak-to-trough ratios (PTR), also a proxy for bacterial cell growth, were calculated and compared between patients with CD and healthy individuals using Mann-Whitney *U* tests ($n = 32$ CD and $n = 63$ healthy controls for the Mayo Clinic study; $n = 13$ CD and $n = 10$ healthy controls for the MetaHIT study). Bacterial species were ranked by the resulting *P* values. (D to F) Analyses of the same datasets as in (A) to (C), but examining relative abundance of bacterial species instead of growth rates/transcriptional activity. (D) Relative abundances were compared to a marker of longitudinal gut dysbiosis for patients with CD ($n = 106$), with the resulting strength of correlation shown on the *y* axis. (E and F) Relative abundances were compared for patients with CD and healthy controls using Mann-Whitney *U* tests on the same individuals as in (B) and (C). (**G**) Count-

based summary of (A) to (C), adding all numbers of each bacterial designation: translocators (yellow), IgG-targeted species (purple), or both IgG-targeted species and translocators (red). Counts of bacterial species are separated by the direction of the trend, as either being enriched or depleted in CD. (**H**) Count summary as in (G) but for relative abundances (D to F).